

Journal Pre-proofs

Novel artemisinin derivatives with potent anticancer activities and the anti-colorectal cancer effect by the mitochondria-mediated pathway

Lan Lin, Wenyu Lu, Tianzhi Dai, Huan Chen, Tong Wang, Li Yang, Xuelian Yang, Ying Liu, Dequn Sun

PII: S0045-2068(20)31794-6
DOI: <https://doi.org/10.1016/j.bioorg.2020.104496>
Reference: YBIOO 104496

To appear in: *Bioorganic Chemistry*

Received Date: 29 August 2020
Revised Date: 24 October 2020
Accepted Date: 20 November 2020

Please cite this article as: L. Lin, W. Lu, T. Dai, H. Chen, T. Wang, L. Yang, X. Yang, Y. Liu, D. Sun, Novel artemisinin derivatives with potent anticancer activities and the anti-colorectal cancer effect by the mitochondria-mediated pathway, *Bioorganic Chemistry* (2020), doi: <https://doi.org/10.1016/j.bioorg.2020.104496>

This is a PDF file of an article that has undergone enhancements after acceptance, such as the addition of a cover page and metadata, and formatting for readability, but it is not yet the definitive version of record. This version will undergo additional copyediting, typesetting and review before it is published in its final form, but we are providing this version to give early visibility of the article. Please note that, during the production process, errors may be discovered which could affect the content, and all legal disclaimers that apply to the journal pertain.

© 2020 Published by Elsevier Inc.



Novel artemisinin derivatives with potent anticancer activities and the anti-colorectal cancer effect by the mitochondria-mediated pathway

Lan Lin ^{1, a, b}, Wenyu Lu ^{1, a, c}, Tianzhi Dai ^{a, c}, Huan Chen ^a, Tong Wang ^a, Li Yang ^a, Xuelian Yang ^a, Ying Liu ^{b, *}, Dequn Sun ^{a, *}

a. School of Life Science and Engineering, Southwest University of Science and Technology, No. 59, Middle Section of Qinglong Avenue, Mianyang 621010, China.

b. Institute of Materials, China Academy of Engineering Physics, Jianguo 621907, China.

c. Marine College, Shandong University at Weihai, No.180, Wenhua West Road, Weihai 264209, P. R. China.

1. two persons contribute this work equally.

* Corresponding author: liuying2016@caep.cn

* Corresponding author: dqsun@swust.edu.cn

Corresponding author:

Ying Liu: liuying2016@caep.cn

Dequn Sun: dqsun@swust.edu.cn

Abstract

Many artemisinin derivatives have good inhibitory effects on malignant tumors. In this work, a novel series of artemisinin derivatives containing piperazine and fluorine groups were designed and synthesized and their structures were confirmed by ¹H-NMR, ¹³C-NMR and HRMS technologies. The in vitro cytotoxicity against various cancer cell lines was evaluated. Among the derivatives, compound **12h** was found to exhibit not only the best activity against HCT-116 cells ($IC_{50} = 0.12 \pm 0.05 \mu M$), but also low toxicity against normal cell line L02 ($IC_{50} = 12.46 \pm 0.10 \mu M$). The mechanisms study revealed that compound **12h** caused the cell cycle arrest in G1 phase, induced apoptosis in a concentration-dependent manner, significantly reduced mitochondrial membrane potential, increased intracellular ROS and Ca²⁺ levels, up-regulated the expression of Bax, cleaved caspase-9, cleaved caspase-3, and down-regulated the expression of Bcl-2 protein. A series of analyses confirmed that **12h** can inhibit HCT-116 cells migration and induce apoptosis by a mechanism of the mitochondria-mediated pathway in the HCT-116 cell line. The present work indicates that compound **12h** may merit further investigation as a potential therapeutic agent for colorectal cancer.

Keywords

Artemisinin derivatives; Piperazine and fluorine groups; Anti-cancer activity; Colorectal cancer; Mitochondria-mediated pathway.

1. Introduction

Artemisinin (ART), a sesquiterpene lactone isolated from *Artemisia annua*, has been widely used to treat malaria. In 2015, Madam Youyou Tu won the Nobel Prize for her contribution to the development of novel antimalarial drugs, artemisinin and dihydroartemisinin [1]. The bioactivity of artemisinin (**Fig.1**) is closely related to the endoperoxide bridge, which is involved in the production of reactive oxygen species (ROS) and peroxy free radicals, inducing oxidative stress, DNA damage, alkylation of target proteins and cell apoptosis [2]. Besides the antimalarial effects, the artemisinin derivatives exhibit a wide range of biological activities [3], such as antimicrobial [4,5], antiviral [6] and anti-multiple tumor cell lines [7-9]. Artemisinin derivatives have the advantages of low cross-resistance, synergistic effect with traditional chemotherapy anticancer drugs, and low toxicity to normal tissues or cell lines [10]. Over the years, artemisinin has been used as a lead compound for the treatment of cancer. Many studies retain the backbone of the endoperoxide bridge and modify artemisinin at the 10-position carbon [11,12].

Piperazine is an important pharmaceutical intermediate. Piperazine derivatives show broad spectrum of pharmacological activities such as antidepressant, anxiolytic, and antipsychotic [13]. Previously, we found artemisinin derivatives with piperazine groups have good antitumor activity [14]. On the other hand, fluorine is the most abundant halogen in the earth's crust and ranks 13th among all elements [15]. Since the fluorine atom has the strongest electronegativity, its introduction into the active molecules can significantly change the physicochemical properties [16]. In 1957, the anti-metabolite 5-fluorouracil was synthesized for the first time [17]. Since then, the introduction of fluorine atoms or fluorine-containing groups into drug molecules has become an important means of drug modification. Our previous work showed that the introduction of fluorine atoms into sulfur heterocyclic derivatives caused good antitumor activity [18]. Grellepois [19] introduced trifluoromethyl group at the C-10 position of artemisinin, confirming that the compound had good antimalarial activity. We previously, introduced piperazine-containing groups at C-10 position to obtain four new artemisinin derivatives, among which the most active compound had the IC_{50} value of about 4.1 μ M for HepG-2 cell line [14]. Furthermore, Li [20] in our group introduced fluorine atoms into piperazine-containing groups to synthesize a new kind of artemisinin derivatives, among which the IC_{50} value of the most active compound was about 2.1 μ M for MCF-7 cell line. Compared with the original designed derivatives, the activity of the derivative was improved. Zhang [21] synthesized five-membered cyclic artemisinin dimers with potent anticancer activity. They retained the endoperoxide bridge and obtained a compound with good activity on PC12 cell line, but it is uncertain whether the five-membered cyclic artemisinin containing piperazine and fluorine groups have good antitumor activity.

Although artemisinin derivatives showed strong anti-tumor potential, its targets are diverse and exact antitumor mechanisms have not yet been elucidated. It has been found that artemisinin drugs can inhibit tumor cell proliferation, induce cell cycle

arrest [22], inhibit tumor cell invasion and metastasis [23], promote tumor cell apoptosis, and induce cell death through the mitochondrial pathway [24]. In the latest research on the anti-tumor activity of artemisinin derivatives, Wang's group reported a series of new compounds with good activity against colorectal cancer cell line (HCT-116), and the IC_{50} value of the most active compound was about $0.110 \mu\text{M}$ [25], although the toxicity and anti-tumor mechanisms were not explored. Krishna's team reported an oral artesunate neoadjuvant therapy with good tolerance in a randomized double-blind pilot clinical phase II trial to treat colorectal cancer (CRC), indicating that ART derivatives could possibly be developed as an anti-CRC drug [26]. In addition, Yu's group synthesized a series of dihydroartemisinin piperazine dithiocarbamate derivatives with prominent inhibitory activity (its IC_{50} was about 25 nM) against human liver cancer cell line [7], but for normal liver cells, its selectivity is unsatisfactory.

In this work, we attempted to design and synthesize a novel series of artemisinin derivatives containing both piperazine and fluorine groups in order to find leading compounds with strong bioactivity and low toxicity. We also exploited the mechanisms so as to explore their potentials as the anti-cancer drug candidates for clinical research.

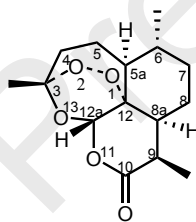
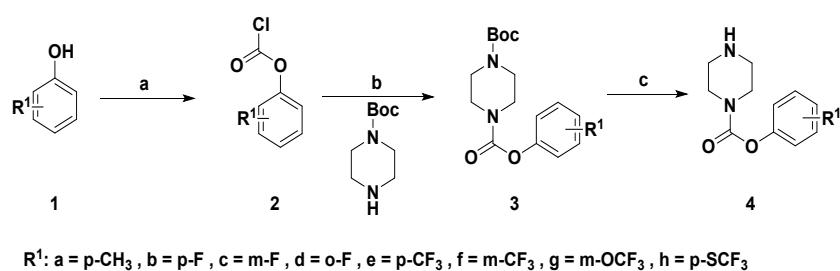


Fig.1. The structure of artemisinin.

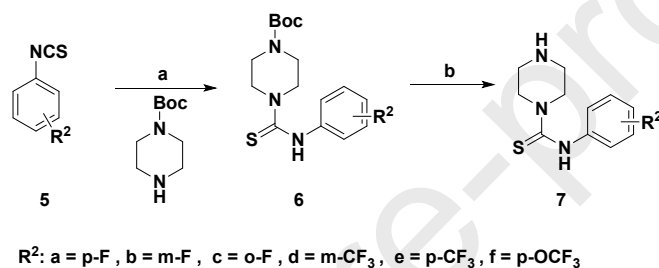
2. Results and Discussion

2.1. Chemistry

Our investigation commenced with the synthesis of phenyl piperazine-1-carboxylate **4** and N-phenylpiperazine-1-carbothioamide **7** (**Scheme 1 and 2**). Commercially available phenols were treated with triphosgene (BTC) and trimethylamine to give the aryl chloroformate **2** [27,28], which was treated with Boc-protected piperazine to obtain 1-(*tert*-butyl) 4-phenyl piperazine-1,4-dicarboxylate **3** [29]. Next, the deprotection of Boc group of **3** with trifluoroacetic acid (TFA) provided desired intermediate **4** [30,31], which was used to synthesize the target compounds **12a-12h** and **18a-18h**. Commercially available aryl isothiocyanates were treated with Boc-protected piperazine to obtain *tert*-butyl 4-(phenylcarbamothioyl)piperazine-1-carboxylate **6** [32]. Next, the deprotection of Boc group of **6** with trifluoroacetic acid (TFA) afforded desired intermediate **7** [30,31], which was used to synthesize the target compounds **13a-13e** and **19a-19e**.



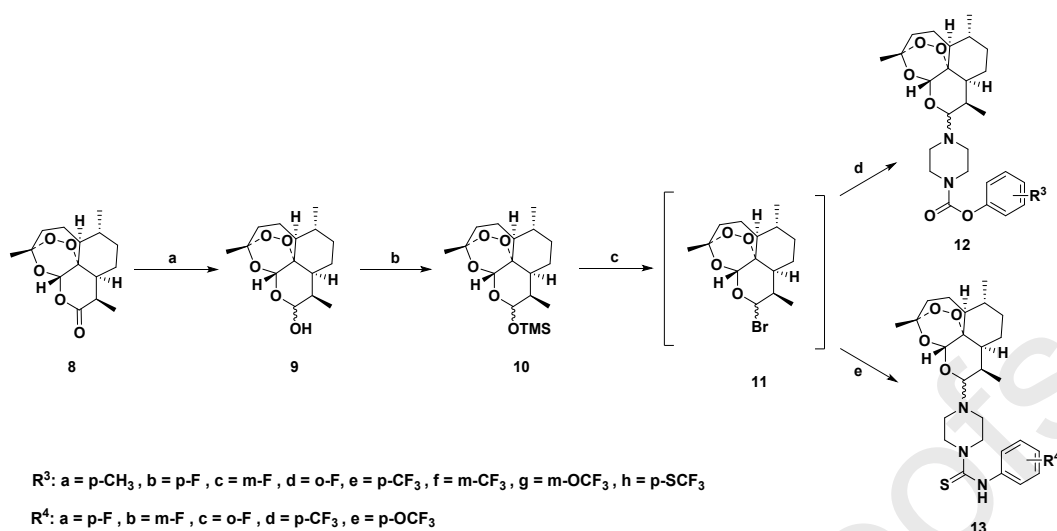
Scheme 1. The synthetic routes of phenyl piperazine-1-carboxylates **4a-4h**. Reagents and conditions: (a) BTC (0.33 equiv), TEA (1 equiv), DCM, 0°C to r.t.; (b) TEA (1.1 equiv), DCM, r.t., 47-64%; (c) TFA : DCM=1:4, 0°C to r.t.



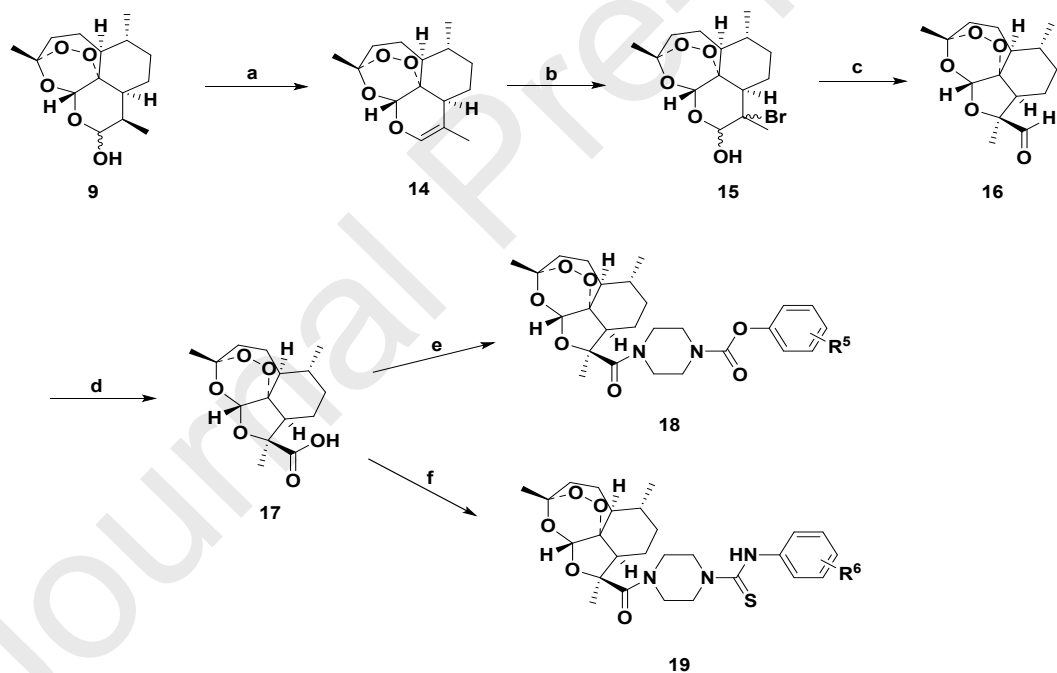
Scheme 2. The synthetic routes of N-phenylpiperazine-1-carbothioamides **7a-7f**. Reagents and conditions: (a) DCM, r.t., 85-99.6%; (b) TFA: DCM=1:4, 0°C to r.t.

The target compounds **12a-12h** and **13a-13e** were synthesized starting from artemisinin according to the literature procedure (**Scheme 3**). Firstly, artemisinin was subjected to NaBH₄-mediated reduction to afford dihydroartemisinin (DHA). Then, DHA was treated with trimethylchlorosilane and triethylamine in DCM at 0–5°C to generate DHA α -trimethylsilyl ether **10** [20]. DHA α -trimethylsilyl ether **10** reacted with trimethylsilyl bromide (TMSBr) to give intermediate bromide **11** which is then treated with an amine nucleophile to form target compounds **12a-12h** and **13a-13e** [33].

As previously reported [21], the synthesis of glycal **14** was prepared from DHA in the presence of a Lewis acid, typically borontrifluoride-diethyl ether. Hydrobromination of **14** gave the bromoacetal **15** in good yield as a mixture of two diastereoisomers. Bromohydrin **15** underwent rearrangement with trimethylamine, leading to aldehyde **16** as a single isomer in excellent yield. Oxidation of **16** with sodium chlorite afforded the corresponding carboxylic acid **17**. With compound **17** in hand, compounds **18a-18h** and **19a-19e** were prepared (**Scheme 4**). The structures of all the compounds were confirmed by ¹H-NMR, ¹³C-NMR and HRMS (Supplementary materials).



Scheme 3. The synthetic routes of six-membered cyclic carbamate artemisinin derivatives **12a-12h**, **13a-13e**. Reagents and conditions: (a) NaBH₄ (3.0 equiv), MeOH, 0-5°C, 89%; (b) TMSCl (1.2 equiv), TEA (2.0 equiv), DCM, 0°C to r.t., 94%; (c) TMSBr (1.02 equiv), DCM, 0-5°C; (d) amine (0.95 equiv), TEA (2 equiv), DCM, 0°C to r.t., 15-30%; (e) amine (0.95 equiv), TEA (2 equiv), DCM/THF, 0°C to r.t., 24-31%.



Scheme 4. The synthetic routes of five-membered cyclic carbamate artemisinin derivatives **18a-18h**, **19a-19e**. Reagents and conditions: (a) BF₃-Et₂O (10.0 equiv), diethyl ether, 0°C to r.t., 90%; (b) Br₂ (1.5 equiv), CCl₄, H₂O, r.t., 96%; (c) TEA (2.5 equiv), DCM, r.t., 91%; (d) aminosulfonic acid (4.0 equiv), sodium chlorite (4.0 equiv), water/dioxane, r.t., 80%; (e) HATU (1.2 equiv), DIPEA, DCM, r.t., 50-74%; (f) HATU (1.2 equiv), DIPEA, DCM/THF, r.t., 27-45%.

2.2. In vitro anticancer evaluations

Twenty-six novel artemisinin derivatives were evaluated for their antiproliferative activities against human neuroblastoma cancer cells (SH-SY5Y), human lung adenocarcinoma cell (A549), breast cancer cells (MCF-7), pheochromocytoma cells (PC12), human glioblastoma (U87MG), human brain astrocyte tumor (U-118MG), colorectal carcinoma cells (HCT-116) and human normal liver cell line (L02) by MTT assay. The IC_{50} for each compound with respect to these cell lines was calculated and the results were summarized in **Table 1**. These values represent the concentration at which a 50% decrease in cell growth is observed after 72 h incubation at the presence of the drug and compared with the control cells treated with ART and DHA, nerve cells treated with Temozolomide (TMZ), as well as positive control cells treated with doxorubicin (DOX) under the same conditions.

As shown in **Table 1**, the derivatives showed enhanced antitumor activity compared to ART and DHA, and lower cytotoxicity against L02 than DOX. For the first series, compounds **12a-12h** exhibited broad-spectrum antitumor effects on MCF-7, PC12 and HCT-116 cells, with IC_{50} values between 0.12-12.36 μ M. What was more noteworthy was that these compounds exhibited excellent inhibitory effects on HCT-116 cells, with IC_{50} values between 0.12-2.16 μ M. Compound **12h** exhibited the strongest inhibitory activity, with an IC_{50} value of 0.12 μ M, which was far superior to the positive control DOX (1.86 μ M), and less cytotoxic to L02. Therefore compound **12h** was considered for further study. For the second series, some compounds among **13a-13e** showed certain inhibitory effects on MCF-7 and PC12 cells, with the IC_{50} values between 2.59-20.54 μ M. Compared to the first series, the activity was slightly reduced. But it was noteworthy that all the compounds of the second series still showed good effects on HCT-116, with the IC_{50} values between 1.08-6.57 μ M. In the third and fourth series (**18a-18h**, **19a-19e**), compound **18e** displayed moderate antiproliferation activity against PC12, SH-SY5Y and U-118MG cell lines, with the IC_{50} values between 4.50-8.84 μ M, while the IC_{50} values for the other compounds were larger than 10 μ M.

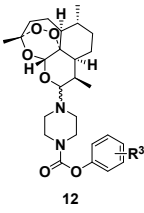
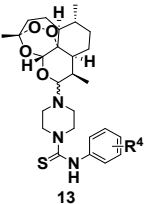
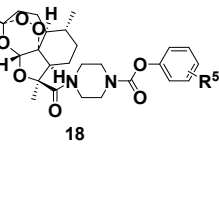
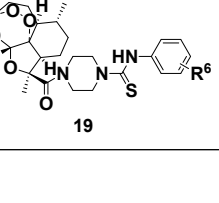
Almost all the compounds tested had no effects on the brain tumor-related cell lines U-118MG and U87MG (the $IC_{50}>40$ μ M), except that **18e** showed an IC_{50} value of 8.14 μ M for U-118MG. This indicated that artemisinin derivatives containing fluorine and piperazine groups had no significant anti-brain tumor effects. Similarly, all the compounds did not show good inhibitory activity on A549 cells. However, for the SH-SY5Y cell line, we were pleasant to find that **12g** exhibited prominent effects with an IC_{50} value of 0.29 μ M, which was equivalent to that of the positive control DOX (0.30 μ M), but the cytotoxicity to L02 is much less than DOX, indicating that **12g** is also a compound worthy of further research.

The structure activity relationship (SAR) studies revealed that the compounds containing both fluorine and piperazine groups have more remarkable activities. Among compounds (**12a**, **12b**, **12d**, **12f**, **12g**, **12h**, **13a**, **13b** and **18e**) with excellent activity ($IC_{50}<10$ μ M), **12a**, **12b**, **12d**, **12f**, **12g**, **12h**, **13a**, **13b** belong to six-membered ring artemisinin derivatives, and only **18e** is five-membered ring

artemisinin derivative. **Table 1** shows that the inhibitory activity of the six-membered ring compounds in each cell line is superior to that of the five-membered ring compound, which may indicate that retaining the six-membered ring structure of artemisinin is necessary to improve the antitumor activity of its derivatives. When we analyzed the selectivity of these compounds for cell lines, we found that all six-membered ring compounds exhibited strong inhibitory activity against HCT-116 cells, indicating that the six-membered ring artemisinin derivatives containing both fluorine and piperazine groups is promising for the treatment of colon cancer cells. Among these compounds, only **13a** and **13b** belong to thiourea derivatives, while the rest are carbamate derivatives. Carbamate derivatives displayed better bioactivity than thiourea derivatives. The derivatives (**18e**, $IC_{50} < 10 \mu M$) containing fluorine groups exhibited better bioactivity than that without fluorine groups (**18a**, $IC_{50} > 40 \mu M$), indicating that fluorine groups in same substituent position could improve the bioactivity of compounds. Moreover, we explored the SAR regarding the substituents on the phenyl ring in each series. For the first series (**12a-12h**), the substitution of fluorine atom both on para (**12b**) and ortho (**12d**) positions exhibited good anticancer activity, especially in HCT-116 cell line, and the substituent on para position (**12b**) displayed low cytotoxicity for L02 cells. The fluorine substituent on meta position (**12c**) decreased the water-solubility of the compound. The trifluoromethoxy group ($-CF_3$) exhibited certain activities in the meta position (**12f**), while poor water solubility in the para position (**12e**). For the second series (**13a-13e**), similarly to compound **12b**, the substitution of fluorine atom on para position (**13a**) showed better activity. Yet, the five-membered ring artemisinin derivative (**18a-18h**) showed opposite results. The substituent of fluorine atom on meta position (**18c**) showed good activity against PC12 cells, but the water-solubility is poor when it was substituted on para position (**18b**). Opposite to **12e**, $-CF_3$ on the para position (**18e**) showed prominent anticancer activity.

It is noted that **12h** and **12g** are two isosteres and similar in their chemical structural formulas. Coincidentally, these two compounds are both candidate compounds that exhibit excellent activity and worthy of further study. Compared with our previous work [14, 20], the activity and selectivity of the trifluoromethylthio ($-SCF_3$) group at the same substituent position are higher than trifluoromethoxy ($-OCF_3$) group, and the compounds with both fluorine and piperazine rings have better antitumor activity than those containing only fluorine or piperazine rings. The results indicate that trifluoromethylthio ($-SCF_3$) group, fluorine and piperazine rings could be meaningful pharmacophores for antitumor activity. In addition, the water-solubility of five-membered ring artemisinin derivatives is opposite to six-membered ring artemisinin derivatives, under the same substituent.

Table 1. Inhibitory activities of **12a-12h**, **13a-13e**, **18a-18h** and **19a-19e** against seven cancer cell lines and one human normal liver cell.

Compound	IC ₅₀ Values (μM) ^a								
	MCF-7	A549	PC12 ^b	SH-SY5Y	U87MG	U-118MG	HCT-116	L02	
 12	12a	3.01±0.36	>40	2.62±0.21	>40	>40	>40	>40	
	12b	12.36±1.51	11.73±0.70	11.10±1.97	>40	>40	>40	0.64±0.12	28.41±1.02
	12c	NT ^c	NT	NT	NT	NT	NT	NT	NT
	12d	6.39±0.66	>40	4.79±1.94	>40	>40	>40	0.65±0.12	14.49±1.20
	12e	NT	NT	NT	NT	NT	NT	NT	NT
	12f	1.81±0.64	>40	5.91±0.71	>40	>40	>40	0.81±0.26	7.15±0.56
	12g	6.08±0.21	>40	2.11±0.38	0.29±0.02	33.12±1.17	24.96±1.19	0.51±0.01	21.03±1.93
	12h	1.96±0.91	>40	>40	4.03±0.11	>40	>40	0.12±0.05	12.46±0.10
 13	13a	4.06±0.94	>40	2.59±0.12	>40	>40	1.08±0.33	2.09±0.51	
	13b	>40	>40	3.61±0.78	>40	33.74±0.97	>40	1.67±0.15	19.54±0.26
	13c	>40	>40	20.54±0.29	32.31±1.02	>40	33.35±0.54	2.73±0.14	>40
	13d	>40	>40	>40	>40	>40	>40	3.69±0.25	15.41±1.41
	13e	>40	>40	>40	>40	>40	>40	6.57±0.31	>40
 18	18a	>40	>40	27.52±0.01	>40	>40	>40	>40	
	18b	NT	NT	NT	NT	NT	NT	NT	NT
	18c	>40	>40	11.08±0.71	>40	>40	>40	>40	>40
	18d	>40	>40	>40	>40	>40	>40	>40	>40
	18e	14.43±0.87	>40	4.51±0.24	8.09±0.01	>40	8.84±0.04	>40	>40
	18f	>40	>40	35.11±0.14	>40	>40	>40	>40	>40
	18g	>40	>40	13.54±0.38	>40	>40	>40	>40	>40
	18h	NT	NT	NT	NT	NT	NT	NT	NT
 19	19a	>40	>40	17.97±0.47	>40	>40	>40	>40	
	19b	>40	>40	30.95±1.97	>40	>40	>40	>40	>40
	19c	>40	>40	>40	>40	>40	>40	>40	>40
	19d	>40	>40	23.33±0.24	>40	>40	>40	32.26±2.13	>40
	19e	>40	>40	>40	>40	>40	>40	>40	>40
ART	>40	>40	>40	>40	>40	>40	>40	>40	
DHA	>40	>40	8.36±0.11	>40	>40	>40	9.11±0.88	9.38±0.13	
DOX	0.35±0.01	0.31±0.13	0.08±0.01	0.30±0.03	NT	NT	1.86±0.12	0.98±0.04	
TMZ	NT	NT	>40	>40	>40	>40	NT	NT	

^a Values are average of three biological replicates and deviation from the average is less than 5% of the average value.

^b NGF-differentiated PC12.

^c NT: not tested. **12c**, **12e**, **18b** and **18h** were not tested because of poor solubility in DMSO.

Next, we carried out selectivity index (SI) analysis to test the selectivity of compound **12h** and **12g**, dividing the IC₅₀ value for L02 by that for cancer cell lines SH-SY5Y and HCT-116. According to the data in **Table 2**, the selectivity of both compounds was better than the positive control DOX. Since the maximum SI of **12h** was 103.83 against HCT-116 cells and was higher than that of **12g** (72.52 against SH-SY5Y cells), compound **12h** was chosen for further mechanisms study. As shown in **Fig. 2**, compound **12h** caused a significant inhibitory effect on the growth of HCT-116 cells. The effect occurred in a concentration- and time-dependent manner.

Table 2. The selectivity of compounds **12g** and **12h** for L02 over the SH-SY5Y and HCT-116 cell lines.

Compound	IC ₅₀ Values (μM)			SI (IC ₅₀ L02/ IC ₅₀ SH-SY5Y)	SI (IC ₅₀ L02/ IC ₅₀ HCT-116)
	SH-SY5Y	HCT116	L02		
12g	0.29±0.07	0.51±0.01	21.03±1.93	72.52	41.24
12h	4.03±0.11	0.12±0.05	12.46±0.10	3.34	103.83
DOX	0.30±0.03	1.86±0.12	0.23±0.03	3.27	0.53

^a Values are average of three biological replicates and deviation from the average is less than 5% of the average value.

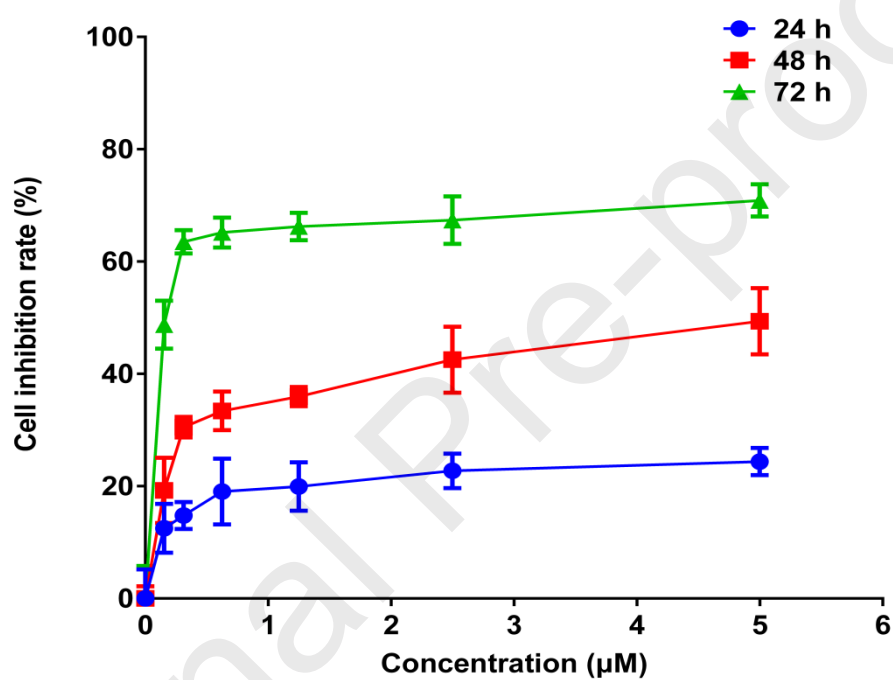


Fig.2. Quantification of inhibitory effects of compound **12h**. Inhibition rate of HCT-116 cells was tested at 24, 48 and 72 h after treatment with compound **12h** (0.1875, 0.375, 0.75, 1.25, 2.5 and 5 μM). Data were expressed as mean \pm SD (n=3).

2.3. Cell cycle arrest induced by compound 12h

Cell-cycle arrest is one of anti-tumor mechanisms. To investigate whether the compound **12h** caused the cell-cycle arrest, the DNA content of cell nuclei was detected by flow cytometry at the indicated time. As shown in **Fig. 3**, compound **12h** led to significant ($P < 0.05$) accumulation of cells at the G1 phase from 49.6% (0 μM) to 70.3% (1 μM), 75.9% (2 μM) and 81.00% (4 μM). The percentage of cells in S and G2 phase were decreased from 28.9% (0 μM) to 6.6% (4 μM) and 21.2% (0 μM) to 11.9% (4 μM), respectively. It is confirmed that the cell DNA replication was inhibited and the cell cycle was arrested in G1 phase by **12h**.

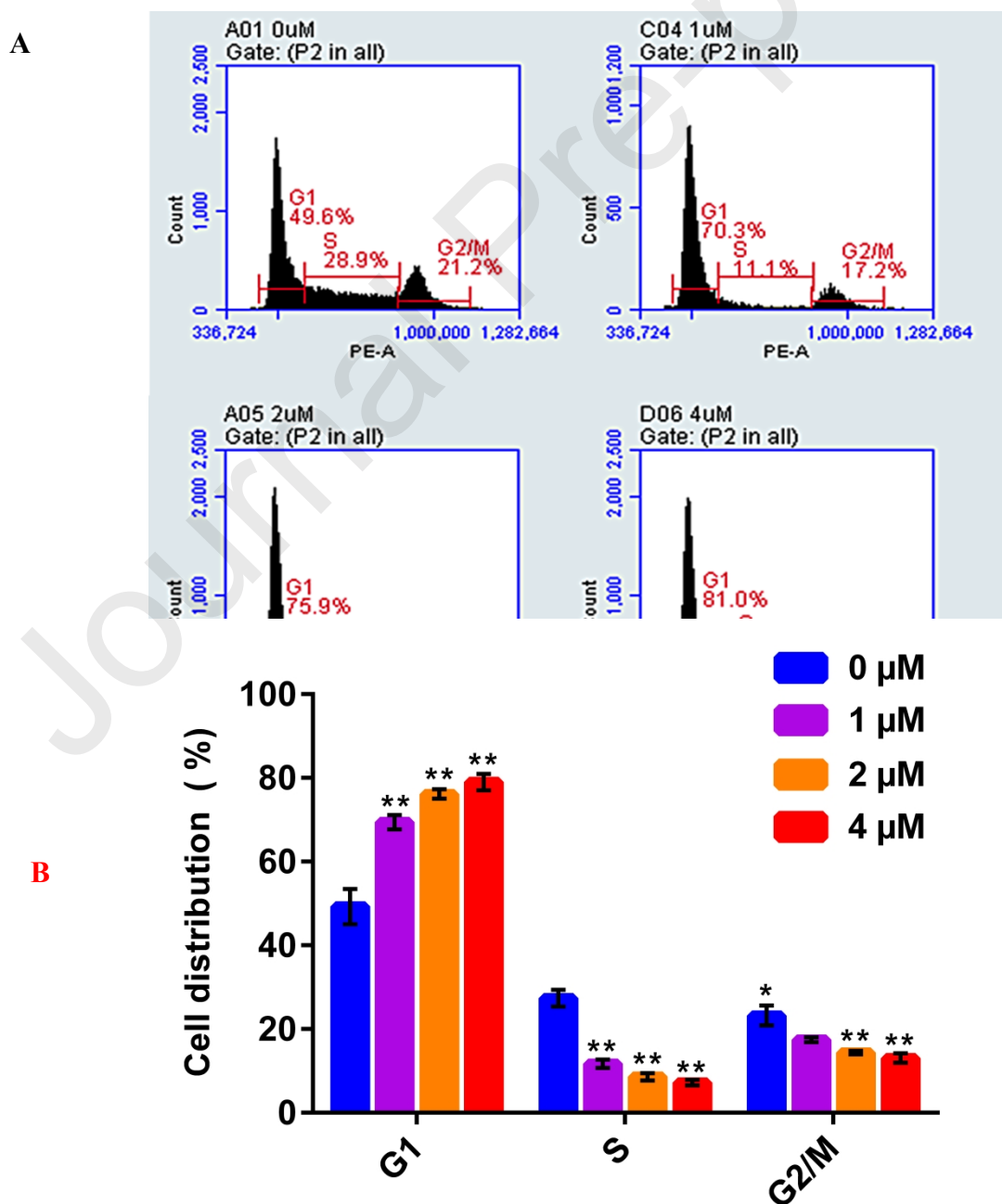
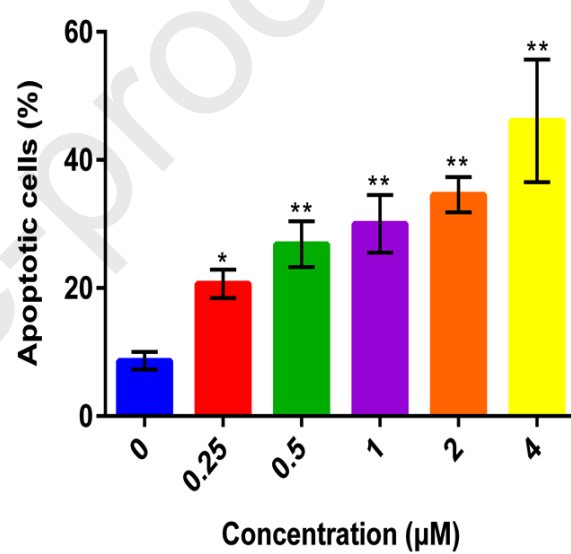
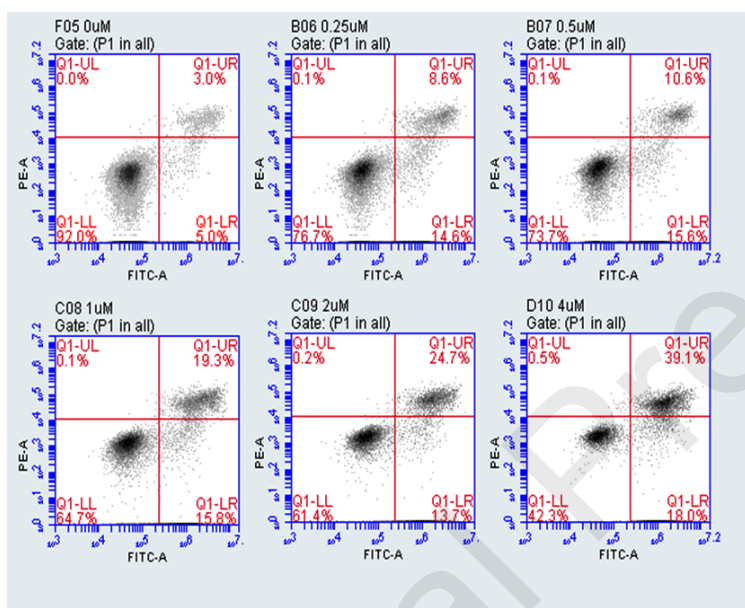


Fig.3. Representative histograms and quantitative analysis showing cell cycle arrest induced by compound **12h**. (A) Cells were treated with 1, 2 and 4 μM of **12h** for 24 h, stained with PI before flow cytometry analysis. (B) The cell distribution rate in G1, S and G2/M phase. Data were expressed as mean \pm SD (n= 3), *P < 0.05, **P < 0.01 versus the controls (0 μM).

2.4. Apoptosis induced by compound **12h**

The induction of cell apoptosis is one of the effective approaches in cancer treatment [34]. Here, we explored whether the anti-colon cancer activity of compound **12h** was associated with apoptosis. As shown in **Fig. 4A**, after treatment with various concentrations of compound **12h**, the percentages of apoptotic cells were 8.0%, 23.2%, 26.2%, 35.1%, 38.4% and 57.1% (Q1UR+Q1LR), respectively, indicating that compound **12h** can induce HCT-116 cells apoptosis and inhibit cells proliferation. Furthermore, Hoechst 33258 was used to stain apoptotic cells immediately. In **Fig. 4B**, HCT-116 cells showed typical apoptosis features such as improved brightness of apoptotic body, cell shrinkage, nuclear condensation (**Fig. 4B** enlarge part). These nuclear morphological changes are different from ferroptosis [35], which mainly damages the mitochondria instead of the nucleus. Our results indicated **12h** probably induced cell death in a different way. The quantitative analysis of apoptotic cells indicated that **12h** induced obvious cell apoptosis in a dose-dependent manner (**Fig. 4A**).

A



B

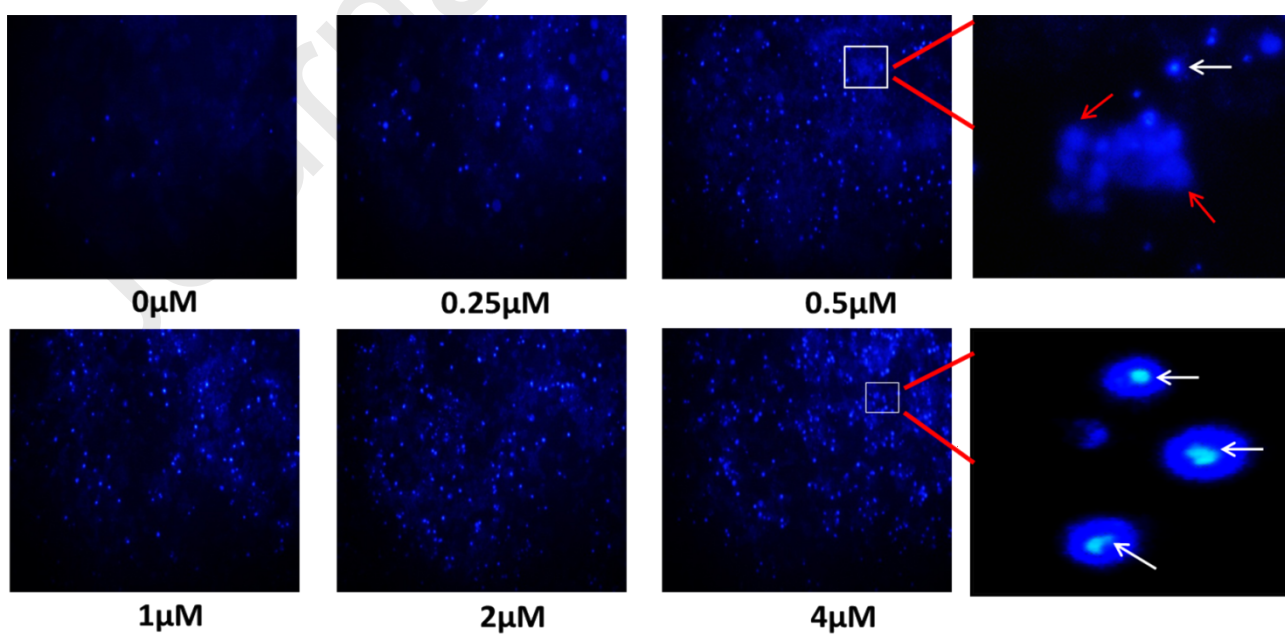


Fig.4. Pro-apoptotic effect of compound **12h** on HCT-116 cell. (A) Representative scatter diagram and quantitative analysis of apoptotic cells (the upper region). HCT-116 cell were treated with compound **12h** at 0, 0.25, 0.5, 1, 2 and 4 μM for 24 h and stained with Annexin V- FITC/PI before flow cytometry analysis. Data were expressed as mean \pm SD (n= 3), *P < 0.05, **P < 0.01 versus the controls (0 μM). (B) Representative microscopy images of HCT-116 cells. Cells were treated with compound **12h** at 0, 0.25, 0.5, 1, 2 and 4 μM for 48 h, stained with Hoechst 33258 and visualized under a fluorescent microscope ($\times 20$). The blue color indicates cell nuclei. Apoptotic bodies are pointed by the white arrows, and normal cells are pointed by the red arrows.

2.5. The change of mitochondrial membrane potential

Mitochondria are involved in a variety of cellular processes and functions, playing a critical role in determining cell survival or death [36]. The change of mitochondrial membrane potential ($\Delta\Psi\text{m}$) is related to cell apoptosis. To verify whether compound **12h** acts on mitochondria, we performed $\Delta\Psi\text{m}$ staining with JC-1, which formed orange fluorescent aggregates and accumulated in the mitochondria of healthy cells. When the $\Delta\Psi\text{m}$ is low, JC-1 produces green fluorescence as a monomer. **Fig. 5A** displays that **12h** induces a decrease of cell population with intense orange fluorescence in a concentration-dependent manner and an accompanying increase of cell population with intense green fluorescence. These data indicate that **12h** causes a loss of $\Delta\Psi\text{m}$, and notably, a rigorous mitochondrial damage response.

We also used the TMRE Mitochondrial Membrane Potential Assay Kit to perform flow cytometry analysis and quantitatively measure $\Delta\Psi\text{m}$. HCT-116 cells treated with **12h** and stained with TMRE. **Fig. 5A** shows that as the concentration increases, the fluorescence intensity decreases, indicating that compound **12h** reduces $\Delta\Psi\text{m}$ in a concentration-dependent manner. All the results prove compound **12h** has a powerful influence on mitochondria, and the anti-tumor effect of compound **12h** maybe through the mitochondrial-mediated apoptosis pathway.

Fig.5. Effects of **12h** on $\Delta\Psi_m$. (A) Representative microscopy images showing in $\Delta\Psi_m$ in HCT-116 cells. Cells were treated with compound **12h** at 0, 0.5, 1 and 2 μM for 48 h, stained with JC-1 and visualized under a fluorescent microscope ($\times 20$). The red color indicates JC-1 gathered in the mitochondria of healthy cells. The green indicates mitochondrial membrane is damaged and JC-1 is released as a monomer. (B) Representative histograms and quantitative analysis showing the change of $\Delta\Psi_m$. HCT-116 cell were treated with compound **12h** at 0, 0.25, 0.5, 1, 2 and 4 μM for 24 h and stained with TMRE before flow cytometry analysis. Data were expressed as mean \pm SD (n= 3). **p <0.01 versus the controls (0 μM).

2.6. Effects on reactive oxygen species (ROS) and intracellular free calcium

The mitochondrial function disturbance is an important event in apoptosis via the mitochondria-mediated pathway, which is commonly involved in the cell death stimuli. It can cause downstream caspase cascade activation and changes of mitochondrial permeability, intracellular Ca^{2+} concentration and ROS level [37]. Using DCFH fluorescence intensity as an index of ROS accumulation, we demonstrated that the cells treated with compound **12h** showed a prominent accumulation of ROS compared to the control cells (0 μM). ROS can initiate oxidative stress and ultimately cause cellular damages, which lead to destructive actions on both DNA and proteins [34]. Therefore, compound **12h** can increase the ROS level and cause oxidative damage to HCT-116 cells.

The FLOU-3 fluorescence was used to test the intracellular free calcium levels. **Fig.6B** showed that **12h** induced a gradual increase in intracellular free Ca^{2+} levels in a concentration-dependent manner. Compared with the ROS levels, the effect of compound **12h** on intracellular free Ca^{2+} levels is more prominent. Therefore, it is most likely that compound **12h** stimulates cells to cause mitochondrial membrane damage. In turn, the $\Delta\Psi_m$ decreases, meanwhile Ca^{2+} and reactive oxygen flow out.

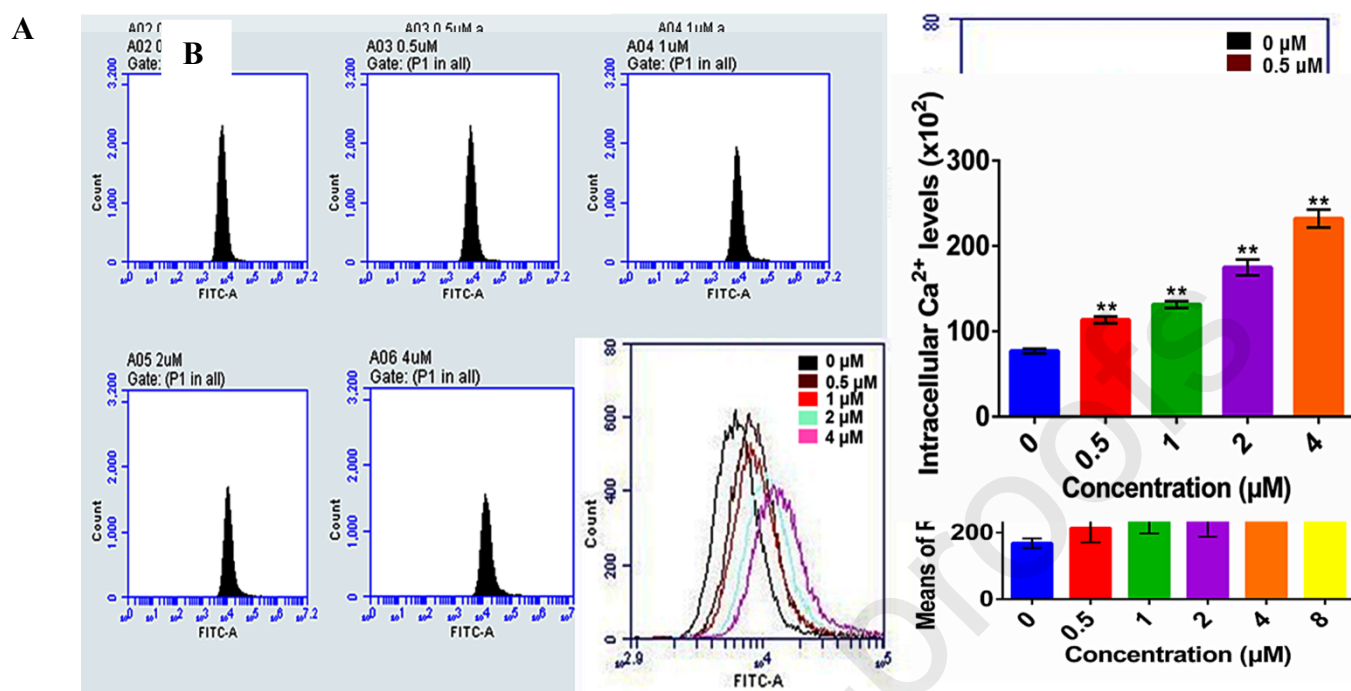
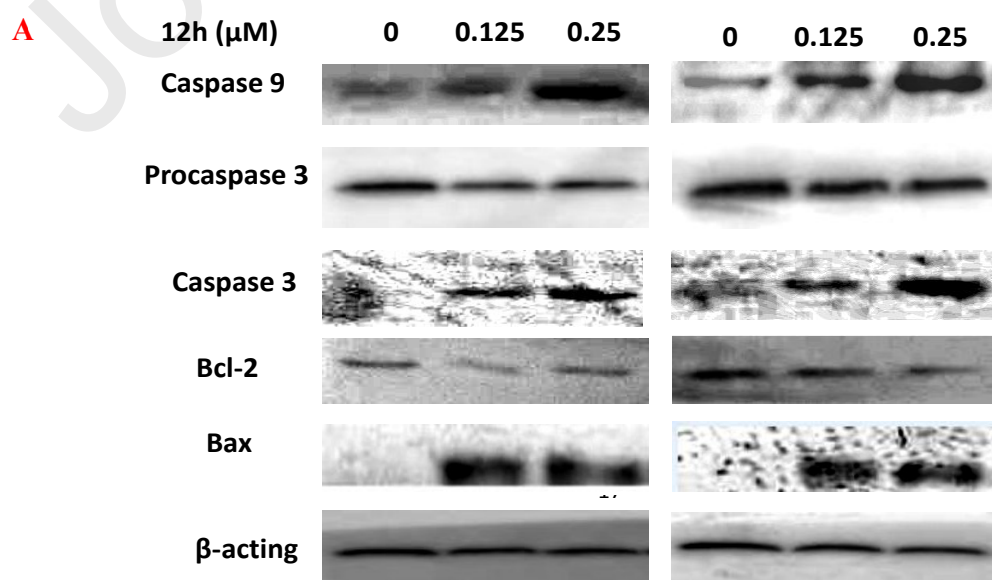


Fig.6. Effects on ROS and intracellular calcium levels. (A) Representative histograms and quantitative analysis indicating ROS levels by flow cytometry. HCT-116 cells treated with **12h** at the concentrations of 0, 0.5, 1, 2, 4 and 8 μM for 12 h and loaded with DCFH-DA fluorescent probe before analysis. (B) Representative histograms and quantitative analysis indicating intracellular free calcium levels by flow cytometry. HCT-116 cells treated with **12h** at the concentrations of 0, 0.5, 1, 2 and 4 μM for 24 h, before the fluorescence of FLOU-3 was determined. ROS or Ca²⁺ levels were represented as the fluorescence intensity. Data were expressed as mean ± SD (n= 3). *p <0.05 and **p <0.01 versus the controls (0 μM).

2.7. Effects of 12h on apoptosis-related proteins

To further explore the potential molecular mechanisms of **12h**-induced apoptosis, the effects of **12h** on the expression level of proteins related with mitochondria mediated apoptosis were examined. It has been demonstrated that BH3-only family proteins play a crucial role in regulating the intrinsic apoptotic pathway. When cells are stimulated by apoptotic factors, BH3-only family in the cytoplasm can sense various apoptotic signals transmitted upstream and activate corresponding protein expressions, including pro-apoptotic proteins (Bax, Bad) and anti-apoptotic proteins (Bcl-2). Bax opens the osmotic transport pores in the mitochondrial membrane, releasing cytochrome C which combines with apoptosis protein activating

factor (Apaf-1) and ATP / dATP to form an apoptosis complex. This complex recruits Pro-caspase-9, leading to the hydrolytic activation of Pro-caspase-9, causing the downstream caspase cascade to activate and induce apoptosis [37]. The expression levels of mitochondrial pathway related proteins in HCT-116 cells pretreated with **12h** are shown in **Fig. 7**. The immunoblot results showed that treatment with compound **12h** decreased Bcl-2 expression and increased Bax in a concentration-dependent manner (**Fig. 7A**). As in **Fig. 7B**, the proportion of Bax/Bcl-2 increased. Since the Bax/Bcl-2 ratio is the "molecular switch" that initiates apoptosis, we can infer that compound **12h** can induce apoptosis by elevating the ratio of Bax/Bcl-2. Compared with the control group, the expressions of cleaved caspase-9 and caspase-3 were also up-regulated, indicating that the mitochondrial pathway is activated. All these molecular expression results indicate that compound **12h** can induce apoptosis of HCT-116 cells through a mitochondrial-mediated pathway.



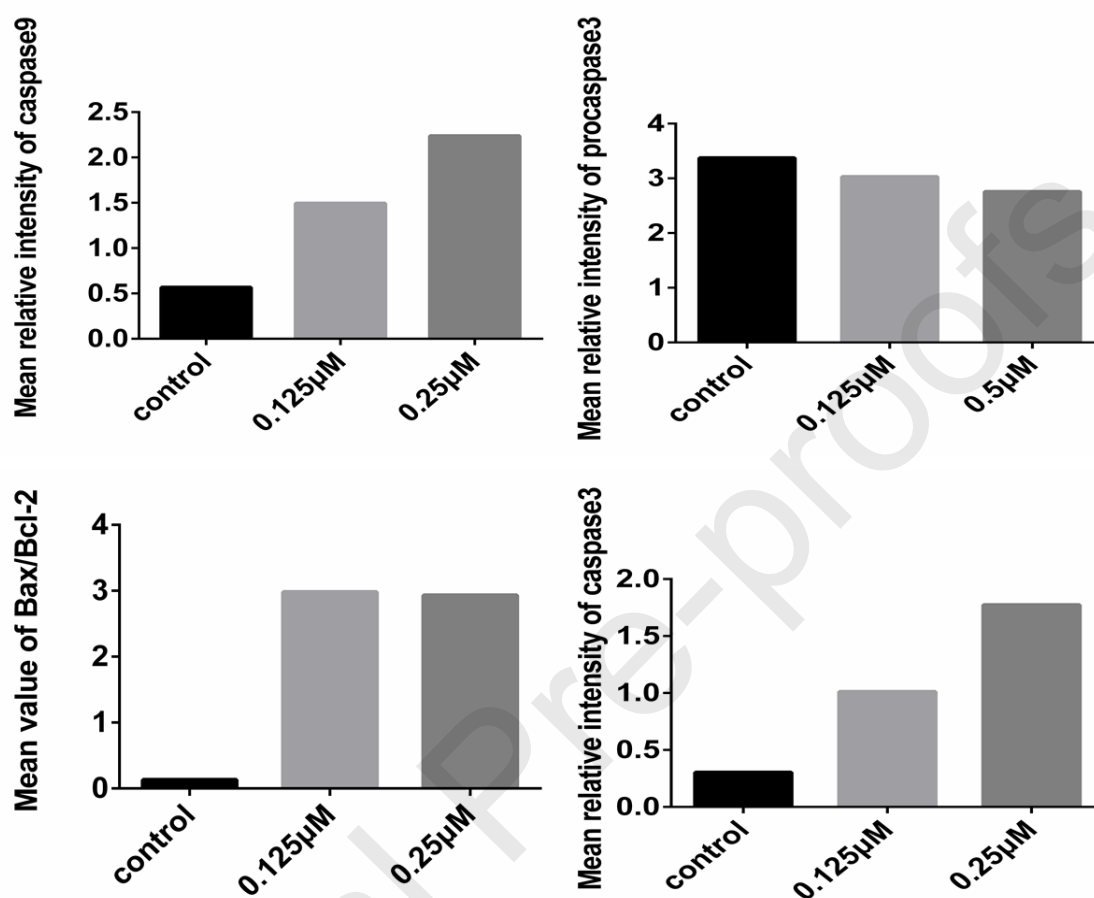
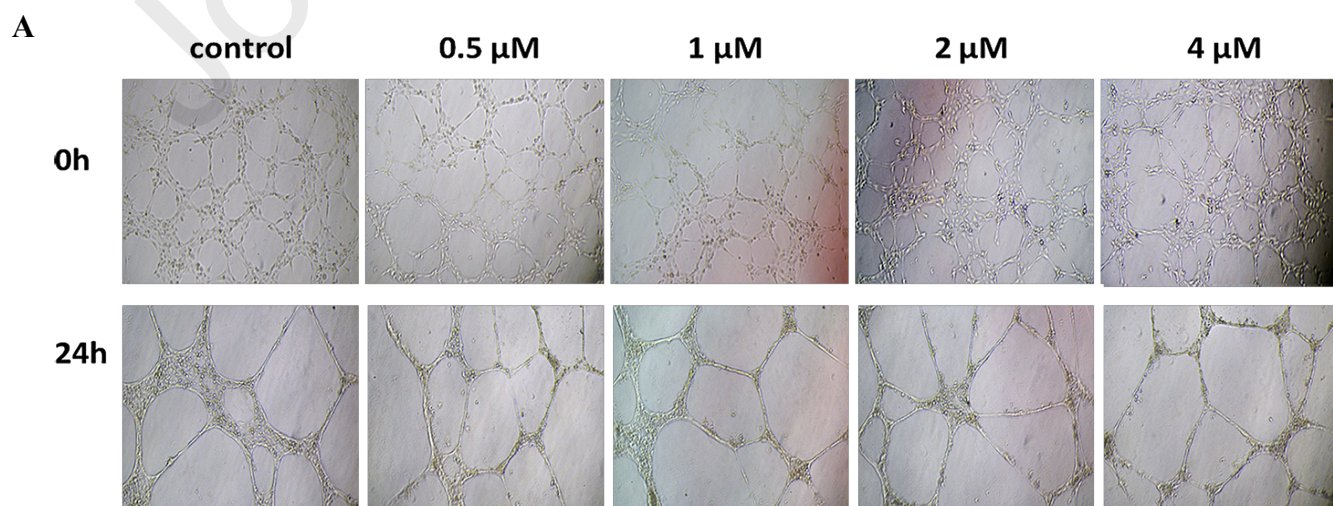


Fig.7. The expression of mitochondrial-mediated pathway related protein in HCT-116 cells. Cells were treated with 0, 0.125 and 0.25 μM of compound **12h** for 48 h and β -actin was used as the internal control. (A) The expression of caspase and Bcl-2 family proteins detected by western blot. (B) The protein levels of caspase-9, procaspase-3, caspase-3, and the rate changes of Bax/Bcl-2 in treated HCT-116 cells. The two panels are independent replicates of the same experiment.

2.8. Effects on tubule morphology and the HCT-116 migration

The establishment of the vascular system is an important process for the growth and survival of tumor cells. The growth of primary tumors and secondary tumor cells requires a continuous supply of nutrients from blood vessels. Most artemisinin derivatives possess vascular disrupting activity, which is thought to disrupt microtubule dynamics to induce the changes in endothelial cell morphology. To evaluate the anti-vascular activity of compound **12h**, we used primary human umbilical vein endothelial cells (HUVEC) culture assay to assess the ability of **12h** to inhibit vascular activity. As shown in **Fig.8A**, after treatment with **12h** for 24 h, we

did not find the number of microtubules reduced (**Fig.8S**) or microtubule disrupted compared with the control group, indicating that compound **12h** did not show anti-vascular activity. Because colorectal cancer is a malignant tumor, easy to metastasize to lymph, liver, lung, bone and other tissues, endangering life safety, we tested the effect of compound **12h** on cell migration. According to the results of the scratch experiment (**Fig. 8B**), **12h** can obviously inhibit the migration of HCT-116 cells, and in turn inhibit the metastasis and spread of colon cancer cells to other tissues. It is promising for clinical treatment of early colorectal cancer.



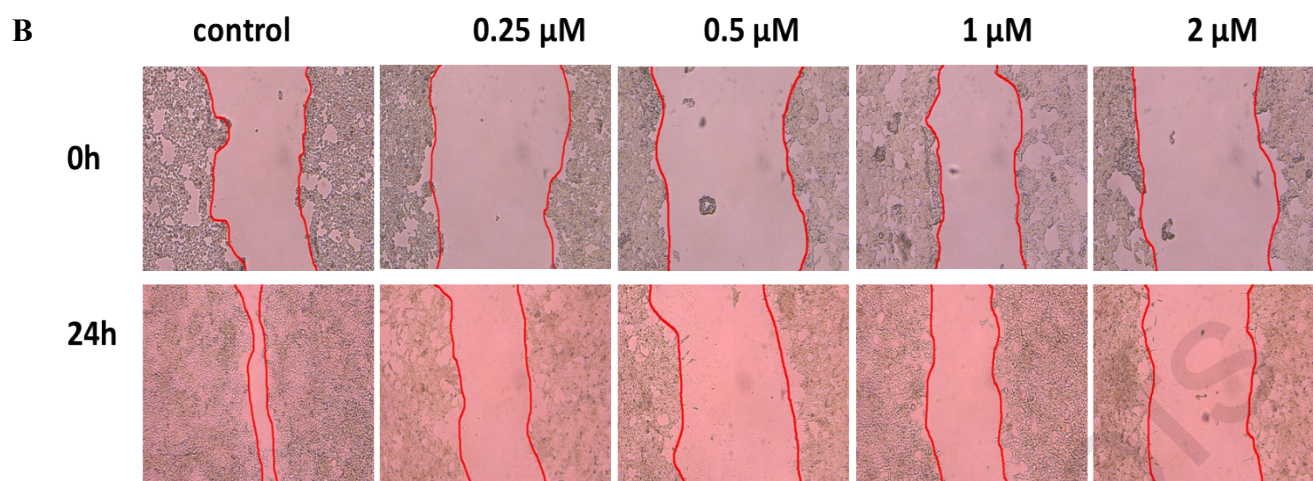


Fig.8. Effects on tube formation and the HCT-116 migration. (A) Images depicting the formation of HUVEC capillary-like tubular network by treatment with **12h** (0, 0.5, 1, 2 and 4 μM) for 24 h. (B) Scratches were created with a sterile 20 μL pipette tip and images were captured at 0 and 24 h after treatment with **12h** (0, 0.25, 0.5, 1 and 2 μM).

3. Conclusion

In summary, a series of novel artemisinin derivatives containing fluorine atoms and piperazine group were synthesized and their cytotoxic activity against seven tumor cell lines and one human normal liver cell line were determined. Compared to ART and DHA, most of derivatives showed improved bioeffects against tumor cell lines and yet less cytotoxicity towards normal cells. The SAR study revealed that six-membered cyclic carbamate derivatives containing both fluorine and piperazine groups tended to have better inhibitory activities. However, the change of artemisinin's six-membered lactone into a five-membered lactone did not increase its activity, and the water-solubility of five-membered ring artemisinin derivatives is opposite to six-membered ring artemisinin derivatives, under the same substituent. In particular, the compound **12h** was the most active derivative and effectively suppressed the tumor growth in vitro with an IC_{50} of 0.12 μM with low cytotoxicity to L02. It also displayed prominent selectivity compared with the control DOX. Its mechanisms of action against HCT-116 cell line was studied and revealed. Compound **12h** could inhibit DNA replication and arrest cell cycle in G1 phase and induce cell apoptosis in a dose-dependent manner. The change of mitochondrial membrane potential proved that **12h** could damage mitochondria and increase the levels of intracellular ROS and Ca^{2+} . Furthermore, **12h** could up-regulate the expression levels of Bax, cleaved caspase-9, cleaved caspase-3 and down-regulate Bcl-2. Compound **12h** did not show the rupture of microtubule, but inhibited the migration of HCT-116 cells. From all above, compound **12h** has a selective and significant anti-cancer activity, inhibiting HCT-116 cells migrate and inducing apoptosis by a mechanism of the mitochondria-mediated pathway. The compound **12h** may merit further

investigation as a potential therapeutic agent for colorectal cancer.

4. Experimental section

4.1. Materials and methods

All chemicals were purchased from commercial source and used without further purification unless otherwise stated. The reactions were monitored by TLC using ultraviolet (UV) light at 254 nm; analytical thin-layer chromatography was carried out on silica gel GF₂₅₄. The products were purified by column chromatography by using silica gel (200-300 mesh). Reagents were all analytically or chemically pure. All the solvents and liquid reagents were dried by standard methods in advance or distilled before use. ¹H NMR spectra were obtained on an Agilent 400MR, Varian 500MR or Bruker Avance 600MR spectrometer at ambient temperature. Data were reported as follows: chemical shift on the δ scale using residual proton solvent as internal standard [δ 0.00 (TMS)], multiplicity (br = broad, s = singlet, d = doublet, t = triplet, q = quartet, m = multiplet), integration, and coupling constant (s) in hertz. ¹³C NMR spectra were obtained with proton decoupling on an Agilent 400MR (100 MHz) or Varian 500MR (125 MHz) spectrometer and were reported in ppm with residual solvent for internal standard [δ 77.16 (CDCl₃)]. The NMR data was processed by software Mest Re-Nova (Ver. 9.0.0.12821, mestrelab research S.L.). High resolution mass spectra were obtained on an Agilent spectrometer. Melting point was determined by WRS-2 Digital Melting Point Apparatus and was uncorrected.

4.2. Chemical synthesis

4.2.1. General procedure for the preparation of aryl chloroformates (2a-2h)

1.0 g (3.37 mmol) BTC was dissolved in 30 mL dry CH₂Cl₂, and cooled in ice bath. 10.11 mmol substituted phenol was slowly added with stirring, then the mixed solution of 10.11 mmol triethylamine and 10 mL dry CH₂Cl₂ was dropped at 0-5°C. The solution was stirred for 1 h at 0-5°C, then stirred for 2 h at room temperature. The crude product was diluted with CH₂Cl₂ and washed with HCl (1 N), saturated NaHCO₃, and finally with saturated NaCl solution. The collected organic layer was dried with Na₂SO₄ and the solvent was removed under vacuum to give the product which was used in the next step without further treatment [27,28].

4.2.2. General procedure for the preparation of 1-(*tert*-butyl) 4-phenyl piperazine-1,4-dicarboxylates (3a-3h)

To the solution of 1-BOC-piperazine (1 g, 5.36 mmol) in dichloromethane (5 mL) and triethylamine (1.1 equiv, 817 μ L) was added compound **2** (1 equiv). The reaction mixture was stirred at room temperature until TLC showed the completion of reaction, the reaction mixture was diluted with CH₂Cl₂, then washed with brine, the organic layer was dried with Na₂SO₄, filtered and evaporated in vacuo to afford crude product which was purified through column chromatography to give compounds **3a-3h** [29].

4.2.2.1. 1-(*tert*-butyl) 4-(*p*-tolyl)piperazine-1,4-dicarboxylate (3a)

The product was obtained as white solid (1.08 g, 63%), m.p.: 145.5-146.4°C. ¹H NMR (400 MHz, Chloroform-d) δ ppm: 7.15 (d, *J* = 8.2 Hz, 2H, Ph-3 and Ph-5), 6.98 (d, *J* = 8.3 Hz, 2H, Ph-2 and Ph-6), 3.57 (d, *J* = 54.0 Hz, 8H, piperazine-H), 2.33 (s, 3H, CH₃), 1.49 (s, 9H, Boc-H) [38].

4.2.2.2. 1-(*tert*-butyl) 4-(4-fluorophenyl)piperazine-1,4-dicarboxylate (3b)

The product was obtained as white solid (0.94 g, 54%), m.p.: 127.7-128.7°C. ¹H NMR (400 MHz, Chloroform-d) δ ppm: 7.09-7.00 (m, 4H, Ph-H), 3.57 (d, *J* = 48.1 Hz, 8H, piperazine-H), 1.49 (s, 9H, Boc-H) [39].

4.2.2.3. 1-(*tert*-butyl) 4-(3-fluorophenyl)piperazine-1,4-dicarboxylate (3c)

The product was obtained as white solid (0.82 g, 47%), m.p.: 65.3-67.5°C. ¹H NMR (400 MHz, Chloroform-d) δ ppm: 7.32 (dd, *J* = 15.0, 8.0 Hz, 1H, Ph-5), 6.96-6.86 (m, 3H, Ph-2 Ph-4 and Ph-6), 3.47 (d, *J* = 48.3 Hz, 8H, piperazine-H), 1.49 (s, 9H, Boc-H) [38].

4.2.2.4. 1-(*tert*-butyl) 4-(2-fluorophenyl)piperazine-1,4-dicarboxylate (3d)

The product was obtained as white solid (0.87 g, 50%), m.p.: 69.7-74.3°C. ¹H NMR (500 MHz, Chloroform-d) δ ppm: 7.19-7.10 (m, 4H, Ph-H), 3.59 (d, *J* = 75.8 Hz, 8H, piperazine-H), 1.48 (s, 9H, Boc-H); ¹³C NMR (125 MHz, Chloroform-d) δ ppm: 154.57 (C=O), 154.47 (d, *J* = 249.0 Hz, Ph-2), 152.71 (C=O), 138.74 (d, *J* = 12.6 Hz, Ph-1), 126.69 (d, *J* = 7.1 Hz, Ph-4), 124.34 (d, *J* = 3.7 Hz, Ph-5), 124.08 (Ph-6), 116.59 (d, *J* = 18.4 Hz, Ph-3), 80.31 (Boc-C), 44.62 (piperazine-C), 44.01 (piperazine-C), 42.98 (piperazine-C), 28.39 (CH₃). HRMS (ESI) Calcd. for [C₁₆H₂₁FN₂O₄Na⁺]: 347.1378, Found, 347.1344.

4.2.2.5. 1-(*tert*-butyl) 4-(4-(trifluoromethyl)phenyl)piperazine-1,4-dicarboxylate (3e)

The product was obtained as white solid (1.10 g, 55%), m.p.: 161.5-168.4°C. ¹H NMR (400 MHz, Chloroform-d) δ ppm: 7.60 (d, *J* = 8.5 Hz, 2H, Ph-3 and Ph-5), 7.21 (d, *J* = 8.4 Hz, 2H, Ph-2 and Ph-6), 3.56 (d, *J* = 52.4 Hz, 8H, piperazine-H), 1.46 (s, 9H, Boc-H); ¹³C NMR (100 MHz, Chloroform-d) δ ppm: 154.49 (C=O), 153.66 (Ph-1), 152.81 (C=O), 127.49 (q, *J* = 32.5 Hz, Ph-C), 126.60 (q, *J* = 3.5 Hz, Ph-C), 123.89 (q, *J* = 270.3 Hz, CF₃), 122.05 (Ph-C), 80.35 (Boc-C), 44.39 (piperazine-C), 43.76 (piperazine-C), 42.79 (piperazine-C), 28.29 (CH₃). HRMS (ESI) Calcd. for [C₁₇H₂₁F₃N₂O₄Na⁺]: 397.1346, Found, 397.1305.

4.2.2.6. 1-(*tert*-butyl) 4-(3-(trifluoromethyl)phenyl)piperazine-1,4-dicarboxylate (3f)

The product was obtained as white solid (1.20 g, 61%), m.p.: 75.2-79.6°C. ¹H NMR (500 MHz, Chloroform-d) δ ppm: 7.49 (d, *J* = 6.8 Hz, 2H, Ph-4 and Ph-6), 7.40 (s, 1H, Ph-2), 7.33 (d, *J* = 6.6 Hz, 1H, Ph-5), 3.59 (d, *J* = 65.9 Hz, 8H, piperazine-H), 1.49 (s, 9H, Boc-H); ¹³C NMR (125 MHz, Chloroform-d) δ ppm: 154.57 (C=O), 153.04 (Ph-1), 151.29 (C=O), 131.84 (q, *J* = 32.9 Hz, Ph-3), 129.87 (Ph-5), 125.29 (Ph-6), 123.57 (q, *J* = 270.6 Hz, CF₃), 122.25 (q, *J* = 3.5 Hz, Ph-C), 119.00 (q, *J* = 3.8 Hz, Ph-C), 80.43 (Boc-C), 44.46 (piperazine-C), 43.86 (piperazine-C), 43.14 (piperazine-C), 28.39 (CH₃). HRMS (ESI) Calcd. for [C₁₇H₂₁F₃N₂O₄Na⁺]: 397.1346, Found, 397.1295.

4.2.2.7. 1-(*tert*-butyl) 4-(3-(trifluoromethoxy)phenyl)piperazine-1,4-dicarboxylate

(3g)

The product was obtained as white solid (1.30 g, 64%), m.p.: 132.6-136.2°C. ¹H NMR (500 MHz, Chloroform-d) δ ppm: 7.38 (t, *J* = 8.3 Hz, 1H, Ph-5), 7.08 (d, *J* = 8.2 Hz, 2H, Ph-4 and Ph-6), 7.04 (s, 1H, Ph-2), 3.58 (d, *J* = 62.1 Hz, 8H, piperazine-H), 1.49 (s, 9H, Boc-H); ¹³C NMR (125 MHz, Chloroform-d) δ ppm: 154.58 (Ph-C), 152.97 (C=O), 151.89 (Ph-C), 149.50 (C=O), 130.00 (Ph-C), 120.40 (q, *J* = 255.9 Hz, OCF₃), 120.21 (Ph-C), 117.80 (Ph-C), 115.00 (Ph-C), 80.42 (Boc-C), 44.46 (piperazine-C), 43.85 (piperazine-C), 43.03 (piperazine-C), 28.39 (CH₃). HRMS (ESI) Calcd. for [C₁₇H₂₁F₃N₂O₅Na⁺]: 413.1295, Found, 413.1285.

4.2.2.8. 1-(*tert*-butyl) 4-(4-((trifluoromethyl)thio)phenyl)piperazine-1,4-dicarboxylate (3h)

The product was obtained as white solid (1.30 g, 60%), m.p.: 110.1-113.1°C. ¹H NMR (500 MHz, Chloroform-d) δ ppm: 7.66 (d, *J* = 8.5 Hz, 2H, Ph-3 and Ph-5), 7.19 (d, *J* = 8.6 Hz, 2H, Ph-2 and Ph-6), 3.58 (d, *J* = 63.4 Hz, 8H, piperazine-H), 1.49 (s, 9H, Boc-H); ¹³C NMR (125 MHz, Chloroform-d) δ ppm: 154.57 (C=O), 153.45 (C=O), 152.85 (Ph-1), 137.68 (Ph-C), 129.45 (q, *J* = 306.5 Hz, SCF₃), 122.78 (Ph-C), 120.86 (Ph-C), 116.54 (Ph-C), 80.46 (Boc-C), 44.49 (piperazine-C), 43.85 (piperazine-C), 42.98 (piperazine-C), 28.39 (CH₃). HRMS (ESI) Calcd. for [C₁₇H₂₁F₃N₂O₄SNa⁺]: 429.1066, Found, 429.1008.

4.2.3. General procedure for the preparation of phenyl piperazine-1-carboxylates (4a-4h)

Trifluoroacetic acid (2.5 mL) was added dropwise into a solution of **3a-3h** (2 mmol) in 10 mL of dichloromethane. The reaction was stirred at room temperature for 1 h. The solvent was removed under vacuum to give residual, then the saturated potassium carbonate solution was added dropwise in an ice bath, and the solution was extracted with dichloromethane (3×20 mL), the organic layer was dried over anhydrous Na₂SO₄, and concentrated under vacuum to obtain the product **4a-4h** [30,31].

4.2.4. General procedure for the preparation of *tert*-butyl 4-(phenylcarbamothioyl) piperazine-1-carboxylate (6a-6f)

To the solution of 1-BOC-piperazine (0.5 g, 2.68 mmol) in dry dichloromethane (20 mL) was added the corresponding isothiocyanate (1.2 equiv). The reaction mixture was stirred at room temperature until TLC showed the completion of reaction, the reaction was diluted with CH₂Cl₂ and then washed with HCl (1 N), saturated NaHCO₃, and finally with saturated NaCl solution. The collected organic layer was dried with Na₂SO₄ and the solvent was removed under vacuum. The compounds were purified by flash chromatography on silica gel using the appropriate eluent [32].

4.2.4.1. *tert*-butyl 4-((4-fluorophenyl)carbamothioyl)piperazine-1-carboxylate (6a)

The product was obtained as white solid (0.90 g, 99.6%), m.p.: 147.4-149.3°C.

¹H NMR (400 MHz, Chloroform-d) δ ppm: 7.15 (dd, $J = 8.8, 4.8$ Hz, 2H, Ph-H), 7.03 (m, 3H, Ph-H, NH), 3.86 (s, 4H, piperazine-H), 3.55 (m, 4H, piperazine-H), 1.46 (s, 9H, Boc-H) [40].

4.2.4.2. *tert*-butyl 4-((3-fluorophenyl)carbamothioyl)piperazine-1-carboxylate (6b)

The product was obtained as white solid (0.84 g, 92%), m.p.: 155.0-158.8°C. ¹H NMR (400 MHz, Chloroform-d) δ ppm: 7.94 (s, 1H, NH), 7.14 (dd, $J = 14.7, 7.6$ Hz, 1H, Ph-H), 6.84 (m, 2H, Ph-H), 6.74 (t, $J = 7.9$ Hz, 1H, Ph-H), 3.69 (s, 4H, piperazine-H), 3.36 (m, 4H, piperazine-H), 1.37 (s, 9H, Boc-H) [40].

4.2.4.3. *tert*-butyl 4-((2-fluorophenyl)carbamothioyl)piperazine-1-carboxylate (6c)

The product was obtained as white solid (0.77 g, 85%), m.p.: 187.3-189.3°C. ¹H NMR (500 MHz, Chloroform-d) δ ppm: 7.57 (t, $J = 6.9$ Hz, 1H, Ph-6), 7.20-7.06 (m, 4H, Ph-H and NH), 3.91 (s, 4H, piperazine-H), 3.56 (m, 4H, piperazine-H), 1.47 (s, 9H, Boc-H); ¹³C NMR (125 MHz, Chloroform-d) δ ppm: 182.86 (C=S), 155.15 (d, $J = 247.8$ Hz, Ph-2), 154.55 (C=O), 127.60 (d, $J = 11.1$ Hz, Ph-5), 126.64 (Ph-4), 126.19 (Ph-6), 124.15 (d, $J = 3.6$ Hz, Ph-1), 115.80 (d, $J = 19.7$ Hz, Ph-3), 80.55 (Boc-C), 48.33 (piperazine-C), 42.94 (piperazine-C), 41.95 (piperazine-C), 28.36 (CH₃). HRMS (ESI) Calcd. for [C₁₆H₂₃FN₃O₂SH⁺]: 340.1490, Found, 340.1487.

4.2.4.4. *tert*-butyl 4-((3-(trifluoromethyl)phenyl)carbamothioyl)piperazine-1-carboxylate (6d)

The product was obtained as white solid (1.00 g, 96%), m.p.: 162.5-163.7°C. ¹H NMR (500 MHz, Chloroform-d) δ ppm: 7.47-7.39 (m, 5H, Ph-H, NH), 3.86 (s, 4H, piperazine-H), 3.54 (m, 4H, piperazine-H), 1.47 (s, 9H, Boc-H); ¹³C NMR (125 MHz, Chloroform-d) δ ppm: 183.10 (C=S), 154.54 (C=O), 140.28 (Ph-1), 131.45 (q, $J = 32.8$ Hz, Ph-C), 129.54 (Ph-C), 126.85 (Ph-C), 123.70 (q, $J = 270.8$ Hz, CF₃), 121.90 (q, $J = 3.6$ Hz, Ph-C), 120.09 (q, $J = 3.6$ Hz, Ph-C), 80.67 (Boc-C), 48.69 (piperazine-C), 43.09 (piperazine-C), 42.21 (piperazine-C), 28.36 (CH₃). HRMS (ESI) Calcd. for [C₁₇H₂₂F₃N₃O₂S₂H⁺]: 390.1458, Found, 390.1438.

4.2.4.5. *tert*-butyl 4-((4-(trifluoromethyl)phenyl)carbamothioyl)piperazine-1-carboxylate (6e)

The product was obtained as white solid (1.04 g, 99.2%), m.p.: 174.5-175.4°C. ¹H NMR (400 MHz, Chloroform-d) δ ppm: 7.70 (s, 1H, NH), 7.55 (d, $J = 8.4$ Hz, 2H, Ph-3 and Ph-5), 7.24 (d, $J = 8.3$ Hz, 2H, Ph-2 and Ph-6), 3.83 (s, 4H, piperazine-H), 3.84 (m, 4H, piperazine-H), 1.47 (s, 9H, Boc-H) [40].

4.2.4.6. *tert*-butyl 4-((4-(trifluoromethoxy)phenyl)carbamothioyl)piperazine-1-carboxylate (6f)

The product was obtained as white solid (1.08 g, 99%), m.p.: 185.9-194.8°C. ¹H NMR (500 MHz, Chloroform-d) δ ppm: 7.30 (s, 1H, NH), 7.23-7.17 (m, 4H, Ph-H), 3.86 (s, 4H, piperazine-H), 3.54 (m, 4H, piperazine-H), 1.47 (s, 9H, Boc-H); ¹³C NMR (125 MHz, Chloroform-d) δ ppm: 183.23 (C=S), 154.54 (C=O), 146.32 (Ph-C), 138.27 (Ph-C), 124.98 (Ph-C), 121.66 (Ph-C), 120.43 (q, $J = 255.8$ Hz, OCF₃), 80.63 (Boc-C), 48.61 (piperazine-C), 43.05 (piperazine-C), 41.91 (piperazine-C), 28.36 (CH₃). HRMS (ESI) m/z calcd. for [C₁₇H₂₂F₃N₃O₃SH⁺]: 406.1407, Found, 406.1402.

4.2.5. General procedure for the preparation of N-phenylpiperazine-1-carbothioamides (7a-7f)

Trifluoroacetic acid (2.5 mL) was added dropwise into a solution of **6a-6f** (2 mmol) in 10 mL of dichloromethane. The reaction was stirred at room temperature for 1 h. The solvent was removed under vacuum to give residual, then the saturated potassium carbonate solution was added dropwise in an ice bath, and the solution was extracted with dichloromethane (3×20 mL), the organic layer was dried over anhydrous Na₂SO₄, and concentrated under vacuum to afford the product **7a-7f** [30,31].

4.2.6. General procedure for the preparation of dihydroartemisinin **9**

Artemisinin (5 g, 17.73 mmol) was dissolved in anhydrous methanol (120 mL) and cooled in an ice bath to 0–5°C. To the solution was added sodium borohydride (3 equiv, 2.02 g) in portion within 30 minutes. The mixture was kept stirring for approximately 30 minutes at 0–5°C, neutralized to PH 7.0 using acetic acid, The reaction solution was concentrated to remove most of methanol, diluted with cold water (60 mL) and stirred for 15 min at room temperature. The precipitate was collected, washed with water (3×20 mL) and dried to afford product as white solid, 4.51 g, m.p.: 146.7-148.5°C. yield: 89%. ¹H NMR (500 MHz, Chloroform-d) δ 5.61 (s, 1H, 12a-H), 5.29 (t, *J* = 3.3 Hz, 1H, 10-H), 2.70-2.60 (m, 2H, 6-H and 9-H), 2.38 (td, *J* = 13.6, 4.0 Hz, 1H, 8a-H), 2.07-2.02 (m, 1H, 5a-H), 1.93-1.79 (m, 3H), 1.68-1.62 (m, 1H), 1.56-1.46 (m, 2H), 1.43 (s, 3H, 3-CH₃), 1.41-1.22 (m, 2H), 0.96 (d, *J* = 7.9 Hz, 6H, 6-CH₃ and 9-CH₃) [20].

4.2.7. General procedure for the preparation of trimethyl(((3*R*,5*aS*,6*R*,8*aS*,9*R*,12*R*,12*aR*)-3,6,9-trimethyldecahydro-12*H*-3,12-epoxy[1,2]dioxepino[4,3-*i*]isochromen-10-yl)oxy)silane **10**

To the solution of dihydroartemisinin **9** (1 g, 3.52 mmol) and triethylamine (2 equiv, 0.36 mg) in anhydrous dichloromethane (15 mL) at 0–5°C was added dropwise a cold solution of trimethylchlorosilane (2 equiv, 1.14 g) in anhydrous dichloromethane (30 mL). After 15 minutes, the reaction was kept stirring for approximately 0.5 h at room temperature. Then solvent was removed under vacuum. The white residue was diluted by petroleum ether (30 mL), then the organic layers was washed with H₂O (3×20 mL), dried over anhydrous Na₂SO₄ and concentrated to afford product as white solid, 1.18 g, yield: 94%. m.p.: 85.6-87.7°C. ¹H NMR (500 MHz, Chloroform-d) δ 5.32 (s, 1H, 12a-H), 4.76 (d, *J* = 9.0 Hz, 1H, 10-H), 2.41-2.28 (m, 2H, 6-H and 9-H), 2.01 (td, *J* = 14.5, 3.0 Hz, 1H, 8a-H), 1.91-1.84 (m, 1H, 5a-H), 1.77-1.65 (m, 2H), 1.56-1.43 (m, 2H), 1.41 (s, 3H, 3-CH₃), 1.34-1.21 (m, 3H), 0.95 (d, *J* = 6.2 Hz, 3H, 6-CH₃), 0.86 (d, *J* = 7.2 Hz, 3H, 9-CH₃), 0.19 (s, 9H) [20].

4.2.8. General procedure for the preparation of (3*R*,5*aS*,6*R*,8*aS*,9*R*,10*R*,12*S*,12*aR*)-10-bromo-3,6,9-trimethyldecahydro-12*H*-3,12-epoxy[1,2]dioxepino[4,3-*i*]isochromene **11**

A cold stirred solution of compound **10** (0.2 g, 0.56 mmol) in dichloromethane (5 mL) was treated drop wise with a cold solution of bromotrimethylsilane (1.02 equiv) in dichloromethane (2 mL) at 0°C. After completion (confirmed by TLC), the reaction solution was used in the next step directly without further purification.

4.2.9. General procedure for the preparation of compounds (12a-12h)

A cold stirred solution of amines **4a-4h** (0.95 equiv) in anhydrous dichloromethane (5 mL) was treated drop wise with a cold solution of triethylamine (2 equiv, 0.12 g). The above solution (containing **11**) was transferred to a stirred solution of amines **4a-4h**. The reaction mixture was stirred overnight at room temperature, then diluted by dichloromethane (20 mL), washed with saturated sodium bicarbonate solution (3×30 mL) and water (3×30 mL), dried over anhydrous Na₂SO₄, concentrated under reduced pressure to yield the crude product, which was further purified by chromatography on silica gel to obtain the products **12a-12h**.

4.2.9.1. p-tolyl 4-((3*R*,5*aS*,6*R*,8*aS*,9*R*,12*R*,12*aR*)-3,6,9-trimethyldecahydro-12*H*-3,12-epoxy[1,2]dioxepino[4,3-*i*]isochromen-10-yl)piperazine-1-carboxylate (**12a**)

The product was obtained as white solid (60 mg, 23%), m.p.: 139.0-145.8°C. ¹H NMR (500 MHz, Chloroform-*d*) δ ppm: 7.14 (d, *J* = 8.2 Hz, 2H, Ph-3 and Ph-5), 6.98 (d, *J* = 8.4 Hz, 2H, Ph-2 and Ph-4), 5.29 (s, 1H, 12*a*-H), 4.06 (d, *J* = 10.2 Hz, 1H, 10-H), 3.70-3.48 (m, 4H, piperazine-H), 3.04 (s, 2H, piperazine-H), 2.75-2.69 (m, 2H, piperazine-H), 2.65-2.56 (m, 1H, 9-H), 2.37 (dd, *J* = 14.0, 3.9 Hz, 1H, 6-H), 2.33 (s, 3H, Ph-CH₃), 2.05-1.97 (m, 1H, 8*a*-H), 1.90-1.85 (m, 1H, 5*a*-H), 1.75-1.68 (m, 2H), 1.59-1.43 (m, 3H), 1.41 (s, 3H, 3-CH₃), 1.38-1.20 (m, 3H), 0.95 (d, *J* = 6.3 Hz, 3H, 6-CH₃), 0.84 (d, *J* = 7.1 Hz, 3H, 9-CH₃); ¹³C NMR (125 MHz, Chloroform-*d*) δ ppm: 153.92 (C=O), 149.21 (Ph-1), 134.71 (Ph-4), 129.73 (Ph-2 and Ph-6), 121.48 (Ph-3 and Ph-5), 104.00 (3-C), 91.67 (12*a*-C), 90.84 (10-C), 80.30 (12-C), 51.74 (5*a*-C), 47.32 (piperazine-C), 47.17 (piperazine-C), 45.83 (piperazine-C), 44.85 (piperazine-C), 44.29 (8*a*-C), 37.40 (6-C), 36.33 (4-C), 34.29 (7-C), 28.48 (9-C), 26.03 (3-CH₃), 24.76 (5-C), 21.65 (8-C), 20.83 (Ph-CH₃), 20.29 (6-CH₃), 13.50 (9-CH₃). HRMS (ESI) *m/z* calcd. for [C₂₇H₃₈N₂O₆H⁺]: 487.2803, Found, 487.2830.

4.2.9.2. 4-fluorophenyl 4-((3*R*,5*aS*,6*R*,8*aS*,9*R*,12*R*,12*aR*)-3,6,9-trimethyldecahydro-12*H*-3,12-epoxy[1,2]dioxepino[4,3-*i*]isochromen-10-yl)piperazine-1-carboxylate (**12b**)

The product was obtained as white solid (74 mg, 28%), m.p.: 120.9-125.1°C. ¹H NMR (400 MHz, Chloroform-*d*) δ ppm: 7.09-6.98 (m, 4H, Ph-H), 5.30 (s, 1H, 12*a*-H), 4.07 (d, *J* = 10.2 Hz, 1H, 10-H), 3.70-3.49 (m, 4H, piperazine-H), 3.04 (s, 2H, piperazine-H), 2.76-2.67 (m, 2H, piperazine-H), 2.64-2.56 (m, 1H, 9-H), 2.35 (td, *J* = 13.9, 3.9 Hz, 1H, 6-H), 2.06-1.98 (m, 1H, 8*a*-H), 1.91-1.83 (m, 1H, 5*a*-H), 1.77-1.67 (m, 2H), 1.59-1.45 (m, 2H), 1.41 (s, 3H, 3-CH₃), 1.37-1.22 (m, 4H), 0.96 (d, *J* = 6.1 Hz, 3H, 6-CH₃), 0.84 (d, *J* = 7.1 Hz, 3H, 9-CH₃); ¹³C NMR (100 MHz, Chloroform-*d*) δ ppm: 159.86 (d, *J* = 242.0 Hz, Ph-4), 153.52 (C=O), 147.21 (Ph-1), 123.15 (d, *J* = 9.0 Hz, Ph-2 and Ph-6), 115.79 (d, *J* = 23.0 Hz, Ph-3 and Ph-5), 103.96 (3-C), 91.63 (12*a*-C), 90.74 (10-C), 80.26 (12-C), 51.66 (5*a*-C), 47.34 (piperazine-C), 47.06 (piperazine-C), 45.75 (piperazine-C), 44.82 (piperazine-C), 44.30 (8*a*-C), 37.36

(6-C), 36.26 (4-C), 34.22 (7-C), 28.43 (9-C), 26.03 (3-CH₃), 24.71 (5-C), 21.61 (8-C), 20.30 (6-CH₃), 13.51 (9-CH₃). HRMS (ESI) *m/z* calcd. for [C₂₆H₃₅FN₂O₆H⁺]: 491.2552, Found, 491.2547.

4.2.9.3. 3-fluorophenyl 4-((3*R*,5*aS*,6*R*,8*aS*,9*R*,12*R*,12*aR*)-3,6,9-trimethyldecahydro-12*H*-3,12-epoxy[1,2]dioxepino[4,3-*i*]isochromen-10-yl) piperazine-1-carboxylate (12c)

The product was obtained as white solid (53 mg, 21%), m.p.: 118.3-121.1°C. ¹H NMR (500 MHz, Chloroform-*d*) δ ppm: 7.30 (dd, *J* = 14.8, 8.0 Hz, 1H, Ph-5), 6.93-6.86 (m, 3H, Ph-2, Ph-4 and Ph-6), 5.29 (s, 1H, 12*a*-H), 4.07 (d, *J* = 10.2 Hz, 1H, 10-H), 3.70-3.49 (m, 4H, piperazine-H), 3.05 (s, 2H, piperazine-H), 2.76-2.69 (m, 2H, piperazine-H), 2.65-2.56 (m, 1H, 9-H), 2.36 (td, *J* = 14.0, 3.9 Hz, 1H, 6-H), 2.06-1.99 (m, 1H, 8*a*-H), 1.90-1.85 (m, 1H, 5*a*-H), 1.76-1.67 (m, 2H), 1.59-1.44 (m, 2H), 1.41 (s, 3H, 3-CH₃), 1.38-1.20 (m, 4H), 0.96 (d, *J* = 6.3 Hz, 3H, 6-CH₃), 0.84 (d, *J* = 7.2 Hz, 3H, 9-CH₃); ¹³C NMR (125 MHz, Chloroform-*d*) δ ppm: 162.84 (d, *J* = 245.0 Hz, Ph-3), 153.03 (Ph-1), 152.34 (C=O), 129.87 (d, *J* = 9.6 Hz, Ph-5), 117.53 (d, *J* = 2.5 Hz, Ph-6), 112.16 (d, *J* = 21.3 Hz, Ph-4), 109.84 (d, *J* = 24.4 Hz, Ph-2), 104.00 (3-C), 91.66 (12*a*-C), 90.80 (10-C), 80.29 (12-C), 51.73 (5*a*-C), 47.36 (piperazine-C), 47.13 (piperazine-C), 45.81 (piperazine-C), 44.93 (piperazine-C), 44.37 (8*a*-C), 37.41 (6-C), 36.31 (4-C), 34.28 (7-C), 28.47 (9-C), 26.03 (3-CH₃), 24.76 (5-C), 21.64 (8-C), 20.29 (6-CH₃), 13.50 (9-CH₃). HRMS (ESI) *m/z* calcd. for [C₂₆H₃₅FN₂O₆H⁺]: 491.2552, Found, 491.2544.

4.2.9.4. 2-fluorophenyl 4-((3*R*,5*aS*,6*R*,8*aS*,9*R*,12*R*,12*aR*)-3,6,9-trimethyldecahydro-12*H*-3,12-epoxy[1,2]dioxepino[4,3-*i*]isochromen-10-yl) piperazine-1-carboxylate (12d)

The product was obtained as white solid (66 mg, 25%), m.p.: 130.1-131.4°C. ¹H NMR (500 MHz, Chloroform-*d*) δ ppm: 7.22-7.05 (m, 4H, Ph-H), 5.30 (s, 1H, 12*a*-H), 4.07 (d, *J* = 10.2 Hz, 1H, 10-H), 3.70-3.49 (m, 4H, piperazine-H), 3.05 (s, 2H, piperazine-H), 2.76-2.70 (m, 2H, piperazine-H), 2.65-2.56 (m, 1H, 9-H), 2.35 (td, *J* = 14.0, 3.9 Hz, 1H, 6-H), 2.04-1.97 (m, 8*a*-H), 1.91-1.84 (m, 1H, 5*a*-H), 1.76-1.66 (m, 2H), 1.61-1.44 (m, 3H), 1.41 (s, 3H, 3-CH₃), 1.38-1.19 (m, 3H), 0.96 (d, *J* = 6.3 Hz, 3H, 6-CH₃), 0.84 (d, *J* = 7.1 Hz, 3H, 9-CH₃); ¹³C NMR (125 MHz, Chloroform-*d*) δ ppm: 154.59 (d, *J* = 246.3 Hz, Ph-2), 152.65 (C=O), 138.93 (Ph-1), 126.38 (d, *J* = 7.0 Hz, Ph-C), 124.23 (Ph-C), 116.50 (d, *J* = 14.2 Hz, Ph-C), 103.99 (3-C), 91.65 (12*a*-C), 90.83 (10-C), 80.28 (12-C), 51.73 (5*a*-C), 47.34 (piperazine-C), 47.20 (piperazine-C), 45.82 (piperazine-C), 45.05 (piperazine-C), 44.53 (8*a*-C), 37.40 (6-C), 36.32 (4-C), 34.29 (7-C), 28.48 (9-C), 26.02 (3-CH₃), 24.76 (5-C), 21.64 (8-C), 20.29 (6-CH₃), 13.51 (9-CH₃). HRMS (ESI) *m/z* calcd. for [C₂₆H₃₅FN₂O₆H⁺]: 491.2552, Found, 491.2558.

4.2.9.5. 4-(trifluoromethyl)phenyl 4-((3*R*,5*aS*,6*R*,8*aS*,9*R*,12*R*,12*aR*)-3,6,9-trimethyldecahydro-12*H*-3,12-epoxy[1,2]dioxepino[4,3-*i*]isochromen-10-yl) piperazine-1-carboxylate (12e)

The product was obtained as white solid (74 mg, 26%), m.p.: 156.6-162.7°C. ¹H NMR (400 MHz, Chloroform-*d*) δ ppm: 7.62 (d, *J* = 8.5 Hz, 2H, Ph-3 and Ph-5), 7.24 (d, *J* = 8.4 Hz, 2H, Ph-2 and Ph-6), 5.30 (s, 1H, 12*a*-H), 4.08 (d, *J* = 10.3 Hz, 1H,

10-H), 3.68-3.46 (m, 4H, piperazine-H), 3.06 (s, 2H, piperazine-H), 2.75-2.67 (m, 2H, piperazine-H), 2.62-2.55 (m, 1H, 9-H), 2.32 (td, $J = 13.9, 3.9$ Hz, 1H, 6-H), 2.01-1.95 (m, 1H, 8a-H), 1.89-1.81 (m, 1H, 5a-H), 1.74-1.65 (m, 2H), 1.57-1.42 (m, 2H), 1.38 (s, 3H, 3-CH₃), 1.36-1.30 (m, 2H), 1.26-1.20 (m, 2H), 0.96 (d, $J = 6.1$ Hz, 3H, 6-CH₃), 0.84 (d, $J = 7.1$ Hz, 3H, 9-CH₃); ¹³C NMR (100 MHz, Chloroform-d) δ ppm: 153.95 (Ph-1), 152.74 (C=O), 127.24 (q, $J = 32.5$ Hz, Ph-C), 126.53 (q, $J = 3.9$ Hz, Ph-C), 123.97 (q, $J = 270.2$ Hz, CF₃), 122.11(Ph-C), 103.97 (3-C), 91.63 (12a-C), 90.73 (10-C), 80.26 (12-C), 51.65 (5a-C), 47.30 (piperazine-C), 47.04 (piperazine-C), 45.74 (piperazine-C), 44.93 (piperazine-C), 44.36 (8a-C), 37.36 (6-C), 36.25 (4-C), 34.21 (7-C), 28.42 (9-C), 26.02 (3-CH₃), 24.70 (5-C), 21.60 (8-C), 20.28 (6-CH₃), 13.49 (9-CH₃). HRMS (ESI) m/z calcd. for [C₂₇H₃₅F₃N₂O₆H⁺]: 541.2520, Found, 541.2511.

4.2.9.6. 3-(trifluoromethyl)phenyl 4-((3*R*,5*aS*,6*R*,8*aS*,9*R*,12*R*,12*aR*)-3,6,9-trimethyldecahydro-12*H*-3,12-epoxy[1,2]dioxepino[4,3-*i*]isochromen-10-yl) piperazine-1-carboxylate (12f)

The product was obtained as white solid (91 mg, 30%), m.p.: 80.0-81.1°C. ¹H NMR (400 MHz, Chloroform-d) δ ppm: 7.50-7.40 (m, 2H, Ph-4 and Ph-6), 7.40 (s, 1H, Ph-2), 7.32 (d, $J = 7.2$ Hz, 1H, Ph-5), 5.30 (s, 1H, 12a-H), 4.07 (d, $J = 10.2$ Hz, 1H, 10-H), 3.72-3.49 (m, 4H, piperazine-H), 3.06 (s, 2H, piperazine-H), 2.78-2.69 (m, 2H, piperazine-H), 2.67-2.55 (m, 1H, 9-H), 2.35 (td, $J = 13.9, 3.9$ Hz, 1H, 6-H), 2.05-1.98 (m, 1H, 8a-H), 1.91-1.83 (m, 1H, 5a-H), 1.76-1.67 (m, 2H), 1.60-1.45 (m, 2H), 1.40 (s, 3H, 3-CH₃), 1.38-1.31 (m, 2H), 1.29-1.22 (m, 2H), 0.96 (d, $J = 6.1$ Hz, 3H, 6-CH₃), 0.84 (d, $J = 7.2$ Hz, 3H, 9-CH₃); ¹³C NMR (100 MHz, Chloroform-d) δ ppm: 152.90 (Ph-1), 151.47 (C=O), 131.61 (q, $J = 32.8$ Hz, Ph-C), 129.73 (Ph-C), 125.40 (Ph-C), 123.59 (q, $J = 270.7$ Hz, CF₃), 121.93 (q, $J = 3.6$ Hz, Ph-C), 119.04 (q, $J = 3.6$ Hz, Ph-C), 103.97 (3-C), 91.62 (12a-C), 90.73 (10-C), 80.25 (12-C), 51.65 (5a-C), 47.30 (piperazine-C), 47.04 (piperazine-C), 45.74 (piperazine-C), 44.91 (piperazine-C), 44.36 (8a-C), 37.36 (6-C), 36.25 (4-C), 34.21 (7-C), 28.43 (9-C), 26.01 (3-CH₃), 24.71 (5-C), 21.60 (8-C), 20.28 (6-CH₃), 13.49 (9-CH₃). HRMS (ESI) m/z calcd. for [C₂₇H₃₅F₃N₂O₆H⁺]: 541.2520, Found, 541.2546.

4.2.9.7. 3-(trifluoromethoxy)phenyl 4-((3*R*,5*aS*,6*R*,8*aS*,9*R*,12*R*,12*aR*)-3,6,9-trimethyldecahydro-12*H*-3,12-epoxy[1,2]dioxepino[4,3-*i*]isochromen-10-yl) piperazine-1-carboxylate (12g)

The product was obtained as white solid (45 mg, 15%), m.p.: 91.9-93.8°C. ¹H NMR (500 MHz, Chloroform-d) δ ppm: 7.36 (t, $J = 8.2$ Hz, 1H, Ph-5), 7.10-7.02 (m, 3H, Ph-2, Ph-4 and Ph-6), 5.30 (s, 1H, 12a-H), 4.07 (d, $J = 10.2$ Hz, 1H, 10-H), 3.70-3.50 (m, 4H, piperazine-H), 3.05 (s, 2H, piperazine-H), 2.76-2.69 (m, 2H, piperazine-H), 2.65-2.57 (m, 1H, 9-H), 2.34 (td, $J = 14.0, 3.9$ Hz, 1H, 6-H), 2.04-1.99 (m, 1H, 8a-H), 1.91-1.84 (m, 1H, 5a-H), 1.76-1.69 (m, 2H), 1.59-1.46 (m, 2H), 1.41 (s, 3H, 3-CH₃), 1.38-1.30 (m, 2H), 1.21-1.27 (m, 2H), 0.96 (d, $J = 6.3$ Hz, 3H, 6-CH₃), 0.84 (d, $J = 7.2$ Hz, 3H, 9-CH₃); ¹³C NMR (125 MHz, Chloroform-d) δ ppm: 152.88 (Ph-C), 152.18 (Ph-C), 149.45 (C=O), 129.86 (Ph-C), 120.40 (q, $J = 255.9$ Hz, OCF₃), 120.32 (Ph-C), 117.49 (Ph-C), 115.06 (Ph-C), 104.01 (3-C), 91.66 (12a-C), 90.81 (10-C), 80.29 (12-C), 51.73 (5a-C), 47.35 (piperazine-C), 47.10 (piperazine-C), 45.81 (piperazine-C), 44.95 (piperazine-C), 44.40 (8a-C), 37.41

(6-C), 36.32 (4-C), 34.28 (7-C), 28.47 (9-C), 26.03 (3-CH₃), 24.76 (5-C), 21.65 (8-C), 20.29 (6-CH₃), 13.49 (9-CH₃). HRMS (ESI) *m/z* calcd. for [C₂₇H₃₅F₃N₂O₇H⁺]: 557.2469, Found, 557.2458.

4.2.9.8. 4-((trifluoromethyl)thio)phenyl 4-((3*R*,5*aS*,6*R*,8*aS*,9*R*,12*R*,12*aR*)-3,6,9-trimethyldecahydro-12*H*-3,12-epoxy[1,2]dioxepino[4,3-*i*]isochromen-10-yl) piperazine-1-carboxylate (12h)

The product was obtained as white solid (70 mg, 25%), m.p.: 149.2-153.5°C. ¹H NMR (500 MHz, Chloroform-*d*) δ ppm: 7.64 (d, *J* = 8.5 Hz, 2H, Ph-3 and Ph-5), 7.19 (d, *J* = 8.6 Hz, 2H, Ph-2 and Ph-6), 5.30 (s, 1H, 12*a*-H), 4.07 (d, *J* = 10.2 Hz, 1H, 10-H), 3.72-3.50 (m, 4H, piperazine-H), 3.05 (s, 2H, piperazine-H), 2.77-2.69 (m, 2H, piperazine-H), 2.65-2.57 (m, 1H, 9-H), 2.35 (td, *J* = 14.0, 3.9 Hz, 1H, 6-H), 2.04-1.98 (m, 1H, 8*a*-H), 1.91-1.84 (m, 1H, 5*a*-H), 1.76-1.67 (m, 2H), 1.58-1.43 (m, 3H), 1.40 (s, 3H, 3-CH₃), 1.38-1.19 (m, 3H), 0.96 (d, *J* = 6.3 Hz, 3H, 6-CH₃), 0.84 (d, *J* = 7.1 Hz, 3H, 9-CH₃); ¹³C NMR (125 MHz, Chloroform-*d*) δ ppm: 153.76 (C=O), 152.74 (Ph-1), 137.62 (Ph-C), 133.11 (Ph-C), 129.47 (q, *J* = 306.3 Hz, SCF₃), 122.86 (Ph-C), 120.40 (Ph-C), 104.01 (3-C), 91.67 (12*a*-C), 90.81 (10-C), 80.29 (12-C), 51.73 (5*a*-C), 47.35 (piperazine-C), 47.12 (piperazine-C), 45.81 (piperazine-C), 44.99 (piperazine-C), 44.41 (8*a*-C), 37.41 (6-C), 36.31 (4-C), 34.28 (7-C), 28.47 (9-C), 26.04 (3-CH₃), 24.75 (5-C), 21.65 (8-C), 20.29 (6-CH₃), 13.49 (9-CH₃). HRMS (ESI) Calcd. for [C₂₇H₃₅F₃N₂O₆SH⁺]: 573.2241, Found, 573.2216.

4.2.10. General procedure for the preparation of compounds (13a-13e)

A cold stirred solution of amines **7a-7c**, **7e-7f** (0.95 equiv) in anhydrous tetrahydrofuran (5 mL) was treated drop wise with a cold triethylamine (2 equiv, 0.12 g). The above solution (containing **11**) was transferred to a stirred solution of amines **7a-7c**, **7e-7f**. The reaction mixture was stirred overnight at room temperature, then concentrated under reduced pressure and the residual was diluted by dichloromethane (30 mL), then washed with saturated sodium bicarbonate solution (3×30 mL) and water (3×30 mL), dried over anhydrous Na₂SO₄, concentrated under reduced pressure to yield the crude product, which was purified by chromatography on silica gel to obtain the products **13a-13e**.

4.2.10.1. *N*-(4-fluorophenyl)-4-((3*R*,5*aS*,6*R*,8*aS*,9*R*,12*R*,12*aR*)-3,6,9-trimethyldecahydro-12*H*-3,12-epoxy[1,2]dioxepino[4,3-*i*]isochromen-10-yl) piperazine-1-carbothioamide (13a)

The product was obtained as white solid (67 mg, 31%), m.p.: 204.4-207.2°C. ¹H NMR (400 MHz, Chloroform-*d*) δ ppm: 7.15 (t, *J* = 8.6 Hz, 2H, Ph-2 and Ph-6), 7.02 (t, *J* = 8.6 Hz, 2H, Ph-3 and Ph-5), 5.28 (s, 1H, 12*a*-H), 4.07 (d, *J* = 10.6 Hz, 1H, 10-H), 3.86 (s, 4H, piperazine-H), 3.04 (dt, *J* = 11.0, 5.0 Hz, 2H, piperazine-H), 2.76 (dt, *J* = 11.0, 5.0 Hz, 2H, piperazine-H), 2.58-2.51 (m, 1H, 9-H), 2.33 (td, *J* = 14.0, 3.8 Hz, 1H, 6-H), 2.04-1.98 (m, 1H, 8*a*-H), 1.92-1.83 (m, 1H, 5*a*-H), 1.75-1.68 (m, 2H), 1.57-1.41 (m, 2H), 1.39 (s, 3H, 3-CH₃), 1.34-1.27 (m, 2H), 1.26-1.18 (m, 2H), 0.95 (d, *J* = 6.1 Hz, 3H, 6-CH₃), 0.82 (d, *J* = 7.1 Hz, 3H, 9-CH₃); ¹³C NMR (100 MHz, Chloroform-*d*) δ ppm: 182.51 (C=S), 160.23 (d, *J* = 245.0 Hz, Ph-4), 135.96 (d, *J* = 3.0 Hz, Ph-1), 126.44 (d, *J* = 8.3 Hz, Ph-2 and Ph-6), 115.64 (d, *J* = 22.7 Hz, Ph-3 and

Ph-5), 104.00 (3-C), 91.57(12a-C), 90.34 (10-C), 80.30 (12-C), 51.60 (5a-C), 49.18 (piperazine-C), 46.80 (piperazine-C), 45.69 (8a-C), 37.34 (6-C), 36.24 (4-C), 34.17 (7-C), 28.52 (9-C), 25.99 (3-CH₃), 24.68 (5-C), 21.59 (8-C), 20.28 (6-CH₃), 13.48 (9-CH₃). HRMS (ESI) m/z calcd. for [C₂₆H₃₆FN₃O₄SH⁺]: 506.2483, Found, 506.2461.

4.2.10.2. *N*-(3-fluorophenyl)-4-((3*R*,5*aS*,6*R*,8*aS*,9*R*,12*R*,12*aR*)-3,6,9-trimethyldecahydro-12*H*-3,12-epoxy[1,2]dioxepino[4,3-*i*]isochromen-10-yl)piperazine-1-carbothioamide (13b)

The product was obtained as white solid (74 mg, 29%), m.p.: 213.9-216.3°C. ¹H NMR (500 MHz, Chloroform-*d*) δ ppm: 7.29-7.24 (m, 1H, Ph-H), 7.15 (s, 1H, NH), 6.93-6.80 (m, 3H, Ph-H), 5.28 (s, 1H, 12a-H), 4.06 (d, *J* = 10.3 Hz, 1H, 10-H), 3.84 (s, 4H, piperazine-H), 3.05 (dt, *J* = 10.8, 4.9 Hz, 2H, piperazine-H), 2.77 (dt, *J* = 11.2, 5.0 Hz, 2H, piperazine-H), 2.59-2.53 (m, 1H, 9-H), 2.34 (td, *J* = 14.0, 3.8 Hz, 1H, 6-H), 2.05-1.98 (m, 1H, 8a-H), 1.90-1.83 (m, 1H, 5a-H), 1.74-1.68 (m, 2H), 1.57-1.44 (m, 2H), 1.39 (s, 3H, 3-CH₃), 1.36-1.29 (m, 2H), 1.27-1.19 (m, 2H), 0.95 (d, *J* = 6.1 Hz, 3H, 6-CH₃), 0.82 (d, *J* = 7.1 Hz, 3H, 9-CH₃); ¹³C NMR (125 MHz, Chloroform-*d*) δ ppm: 182.69 (C=S), 162.99 (d, *J* = 246.2 Hz, Ph-3), 141.67 (d, *J* = 10.3 Hz, Ph-1), 130.20 (d, *J* = 9.3 Hz, Ph-5), 117.93 (d, *J* = 3.0 Hz, Ph-6), 111.60 (d, *J* = 21.2 Hz, Ph-2), 109.79 (d, *J* = 24.4 Hz, Ph-4), 104.03 (3-C), 91.59 (12a-C), 90.46 (10-C), 80.27 (12-C), 51.69 (5a-C), 49.96 (piperazine-C), 46.82 (piperazine-C), 45.76 (8a-C), 37.40 (6-C), 36.30 (4-C), 34.25 (7-C), 28.53 (9-C), 25.99 (3-CH₃), 24.75 (5-C), 21.62 (8-C), 20.28 (6-CH₃), 13.47 (9-CH₃). HRMS (ESI) m/z calcd. for [C₂₆H₃₆FN₃O₄SH⁺]: 506.2483, Found, 506.2473.

4.2.10.3. *N*-(2-fluorophenyl)-4-((3*R*,5*aS*,6*R*,8*aS*,9*R*,12*R*,12*aR*)-3,6,9-trimethyldecahydro-12*H*-3,12-epoxy[1,2]dioxepino[4,3-*i*]isochromen-10-yl)piperazine-1-carbothioamide (13c)

The product was obtained as white solid (56 mg, 21%), m.p.: 126.4-128.5°C. ¹H NMR (500 MHz, Chloroform-*d*) δ ppm: 7.68-7.55 (m, 1H, Ph-H), 7.14-7.07 (m, 3H, Ph-H), 6.97 (s, 1H, NH), 5.28 (s, 1H, 12a-H), 4.08 (d, *J* = 10.2 Hz, 1H, 10-H), 3.91 (s, 4H, piperazine-H), 3.09 (dt, *J* = 11.1, 5.1 Hz, 2H, piperazine-H), 2.81 (dt, *J* = 11.3, 5.1 Hz, 2H, piperazine-H), 2.62-2.54 (m, 1H, 9-H), 2.34 (td, *J* = 14.0, 3.8 Hz, 1H, 6-H), 2.04-1.98 (m, 1H, 8a-H), 1.90-1.83 (m, 1H, 5a-H), 1.74-1.69 (m, 2H), 1.57-1.45 (m, 2H), 1.40 (s, 3H, 3-CH₃), 1.37-1.20 (m, 4H), 0.95 (d, *J* = 6.3 Hz, 3H, 6-CH₃), 0.83 (d, *J* = 7.1 Hz, 3H, 9-CH₃); ¹³C NMR (125 MHz, Chloroform-*d*) δ ppm: 182.18 (C=S), 154.73 (d, *J* = 245.3 Hz, Ph-2), 127.95 (d, *J* = 11.1 Hz, Ph-5), 125.87 (d, *J* = 7.6 Hz, Ph-4), 125.63 (Ph-6), 124.02 (d, *J* = 3.7 Hz, Ph-1), 115.60 (d, *J* = 19.8 Hz, Ph-3), 104.04 (3-C), 91.60 (12a-C), 90.48 (10-C), 80.27 (12-C), 51.70 (5a-C), 49.27 (piperazine-C), 46.85 (piperazine-C), 45.77 (8a-C), 37.41 (6-C), 36.30 (4-C), 34.26 (7-C), 28.55 (9-C), 26.01 (3-CH₃), 24.75 (5-C), 22.66 (8-C), 21.63 (6-CH₃), 13.49 (9-CH₃). HRMS (ESI) m/z calcd. for [C₂₆H₃₆FN₃O₄SH⁺]: 506.2483, Found, 506.2461.

4.2.10.4. *N*-(4-(trifluoromethyl)phenyl)-4-((3*R*,5*aS*,6*R*,8*aS*,9*R*,12*R*,12*aR*)-3,6,9-trimethyldecahydro-12*H*-3,12-epoxy[1,2]dioxepino[4,3-*i*]isochromen-10-yl)piperazine-1-carbothioamide (13d)

The product was obtained as white solid (78 mg, 28%), m.p.: 157.2-161.5°C. ¹H NMR (400 MHz, Chloroform-*d*) δ ppm: 7.56 (d, *J* = 8.4 Hz, 2H, Ph-3 and Ph-5), 7.24

(d, $J = 8.7$ Hz, 3H, NH, Ph-2 and Ph-6), 5.28 (s, 1H, 12a-H), 4.07 (d, $J = 10.2$ Hz, 1H, 10-H), 3.86 (s, 4H, piperazine-H), 3.07 (dt, $J = 10.8$, 4.9 Hz, 2H, piperazine-H), 2.79 (dt, $J = 11.2$, 4.9 Hz, 2H, piperazine-H), 2.60-2.53 (m, 1H, 9-H), 2.34 (td, $J = 13.9$, 3.9 Hz, 1H, 6-H), 2.04-1.98 (m, 1H, 8a-H), 1.90-1.84 (m, 1H, 5a-H), 1.74-1.68 (m, 2H), 1.58-1.44 (m, 2H), 1.39 (s, 3H, 3-CH₃), 1.37-1.20 (m, 4H), 0.95 (d, $J = 6.3$ Hz, 3H, 6-CH₃), 0.82 (d, $J = 7.1$ Hz, 3H, 9-CH₃); ¹³C NMR (125 MHz, Chloroform-d) δ ppm: 182.36 (C=S), 143.13 (Ph-1), 126.27 (q, $J = 32.4$ Hz, Ph-C), 126.26 (q, $J = 3.7$ Hz, Ph-C), 124.05 (q, $J = 270.0$ Hz, CF₃), 121.91 (Ph-C), 104.05 (3-C), 91.60 (12a-C), 90.48 (10-C), 80.27 (12-C), 51.68 (5a-C), 49.92 (piperazine-C), 46.86 (piperazine-C), 45.74 (8a-C), 37.40 (6-C), 36.29 (4-C), 34.24 (7-C), 28.53 (9-C), 26.00 (3-CH₃), 24.74 (5-C), 21.62 (8-C), 20.27 (6-CH₃), 13.48 (9-CH₃). HRMS (ESI) m/z calcd. for [C₂₇H₃₆F₃N₃O₄SH⁺]: 556.2451, Found, 556.2456.

4.2.10.5. *N*-(4-(trifluoromethoxy)phenyl)-4-((3*R*,5*aS*,6*R*,8*aS*,9*R*,12*R*,12*aR*)-3,6,9-trimethyldecahydro-12*H*-3,12-epoxy[1,2]dioxepino[4,3-*i*]isochromen-10-yl)piperazine-1-carbothioamide (13e)

The product was obtained as white solid (69 mg, 24%), m.p.: 139.5-143.4°C. ¹H NMR (500 MHz, Chloroform-d) δ ppm: 7.45-7.32 (m, 4H, Ph-H), 7.13 (s, 1H, NH), 5.28 (s, 1H, 12a-H), 4.07 (d, $J = 10.2$ Hz, 1H, 10-H), 3.87 (s, 4H, piperazine-H), 3.07 (dt, $J = 11.0$, 5.1 Hz, 2H, piperazine-H), 2.79 (dt, $J = 11.3$, 5.1 Hz, 2H, piperazine-H), 2.61-2.52 (m, 1H, 9-H), 2.34 (td, $J = 14.0$, 3.9 Hz, 1H, 6-H), 2.08-1.97 (m, 1H, 8a-H), 1.88 (m, 1H, 5a-H), 1.75-1.68 (m, 2H), 1.58-1.44 (m, 2H), 1.40 (s, 3H, 3-CH₃), 1.37-1.20 (m, 4H), 0.95 (d, $J = 6.3$ Hz, 3H, 6-CH₃), 0.83 (d, $J = 7.1$ Hz, 3H, 9-CH₃); ¹³C NMR (125 MHz, Chloroform-d) δ ppm: 182.42 (C=S), 140.98 (Ph-4), 132.45 (Ph-C), 130.31 (Ph-C), 129.85 (Ph-C), 129.54 (q, $J = 306.4$ Hz, OCF₃), 125.62 (Ph-C), 124.99 (Ph-C), 104.05 (3-C), 91.61 (12a-C), 90.45 (10-C), 80.28 (12-C), 51.70 (5a-C), 49.65 (piperazine-C), 46.85 (piperazine-C), 45.76 (8a-C), 37.41 (6-C), 36.30 (4-C), 34.25 (7-C), 28.55 (9-C), 26.01 (3-CH₃), 24.75 (5-C), 21.63 (8-C), 20.28 (6-CH₃), 13.47 (9-CH₃). HRMS (ESI) m/z calcd. for [C₂₇H₃₆F₃N₃O₅SH⁺]: 572.2401, Found, 572.2360.

4.2.11. General procedure for the preparation of (3*R*,5*aS*,6*R*,8*aS*,12*R*,12*aR*)-3,6,9-trimethyl-3,4,5,5*a*,6,7,8,8*a*-octahydro-12*H*-3,12-epoxy[1,2]dioxepino[4,3-*i*]isochromene 14

Boron trifluoride-diethyl ether (3 mL) was added to a stirred solution of DHA (2.56 g, 9 mmol) at 0°C and the mixture was slowly warmed to room temperature and stirred for 2 h. The reaction solution was subsequently quenched with saturated aqueous NaHCO₃ and dried over anhydrous Na₂SO₄. Filtration and concentration of the filtrate provided a residue which was purified on chromatography to give the product as white solid (2.15 g, 90%), m.p.: 93.6-95.6°C. ¹H NMR (500 MHz, Chloroform-d) δ ppm: 6.19 (s, 1H, 10-H), 5.54 (s, 1H, 12a-H), 2.45-2.36 (m, 1H, 8a-H), 2.09-2.00 (m, 2H), 1.95-1.88 (m, 1H), 1.73-1.63 (m, 2H), 1.59 (s, 3H, 3-CH₃), 1.48-1.44 (m, 1H), 1.42 (d, $J = 2.1$ Hz, 3H, 9-CH₃), 1.31-1.04 (m, 4H), 0.99 (d, $J = 6.5$ Hz, 3H, 6-CH₃) [21].

4.2.12. General procedure for the preparation of (3*R*,5*aS*,6*R*,8*aS*,12*R*,12*aR*)-9-bromo-3,6,9-trimethyldecahydro-12*H*-3,12-epoxy[1,2]dioxepino[4,3-*i*]isochromen-10-ol **15**

To a solution of glycal **14** (2.0 g, 7.5 mmol) in CCl₄ (40 mL) was added dropwise the Br₂ (1 M in CCl₄, 11.3 mL, 11.3 mmol, 1.5 equiv) at 0°C. After 30 min of stirring at this temperature, the distilled water (10 mL) was added and the mixture was stirred for an additional 1 h. The reaction was diluted with Et₂O, the organic layer was washed with sodium thiosulfate aqueous solution, aqueous NaHCO₃, and brine, and then dried over anhydrous Na₂SO₄. Evaporation of the solvent under reduced pressure afforded the bromodihydroartemisinin **15** (2.6 g, 96%) as white solid (a mixture of two isomers), which was used in next step directly [21].

4.2.13. General procedure for the preparation of (3*R*,5*aS*,6*R*,8*aS*,9*S*,11*R*,11*aR*)-3,6,9-trimethyloctahydro-3*H*,11*H*-3,11-epoxy[1,2]dioxepino[3,4-*d*]isobenzofuran-9-carbaldehyde **16**

To a solution of compound **15** (2.5 g, 6.9 mmol) in 150 mL of DCM was added triethylamine (TEA) (17.2 mmol, 2.5 mL, 2.5 equiv). The reaction mixture was stirred at room temperature until completion of the reaction monitored by TLC. The mixture was then treated with HCl (0.6 N) to neutralize excess TEA. The organic layer was washed with NaHCO₃, dried over Na₂SO₄, filtered and concentrated to give crude product which was purified through column chromatography to afford **16** (1.8 g, 91%) as fine, cream-white crystals, m.p.: 101.2-103.4°C. ¹H NMR (500 MHz, Chloroform-*d*) δ ppm: 9.77 (s, 1H, CHO), 5.87 (s, 1H, 12*a*-H), 2.39-2.23 (m, 2H), 2.15-1.99 (m, 2H), 1.79-1.74 (m, 1H), 1.63 (s, 3H, 3-CH₃), 1.60-1.52 (m, 2H), 1.50 (s, 3H, 9-CH₃), 1.48-1.13 (m, 4H), 1.01 (d, *J* = 6.4 Hz, 3H, 6-CH₃) [21].

4.2.14. General procedure for the preparation of (3*R*,5*aS*,6*R*,8*aS*,9*S*,11*R*,11*aR*)-3,6,9-trimethyloctahydro-3*H*,11*H*-3,11-epoxy[1,2]dioxepino[3,4-*d*]isobenzofuran-9-carboxylic acid **17**

To a solution of aldehyde **16** (1.3 g, 4.6 mmol) in 1,4-dioxane (50 mL) was added the solution of amino sulfonic acid (1.8 g, 18.77 mmol) in water (17.5 mL). The mixture was stirred for 20 h at 0°C, then NaClO₂ (1.7 g, 18.77 mmol) and water (12.5 mL) were added. After stirring for 30 min, Na₂SO₃ (1.16 g) was added and the mixture was diluted with water (50 mL). The mixture was extracted with diethyl ether (3×100 mL) and the organic layer was washed with brine, dried over anhydrous Na₂SO₄ and evaporated. The product was obtained as brown solid (1.1 g, 80%), m.p.: 133.0-135.9 °C. ¹H NMR (500 MHz, Chloroform-*d*) δ ppm: 5.79 (s, 1H, 12*a*-H), 2.38-2.27 (m, 2H), 2.09-1.98 (m, 3H), 1.83 (s, 3H, 3-CH₃), 1.63-1.49 (m, 2H), 1.47 (s, 3H, 9-CH₃), 1.46-1.03 (m, 4H), 0.99 (d, *J* = 6.4 Hz, 3H, 6-CH₃) [21].

4.2.15. General procedure for the preparation of compounds (18a-18h)

Compound **17** (0.34 mmol) and HATU (0.41 mmol, 1.2equiv) was dissolved in 10 mL of DCM, and DIPEA (0.18 mmol, 3 equiv) was added to the solution. The mixture was stirred for 1 h at room temperature, then the solution of compounds

4a-4h in anhydrous dichloromethane was added. The reaction mixture was stirred overnight at room temperature, the mixture was diluted with dichloromethane (15 mL) and was extracted with DCM (3×30 mL). The combined organic layer was washed with brine, dried over anhydrous over Na₂SO₄ and evaporated to give crude product which was purified through column chromatography to obtain compounds **18a-18h**.

4.2.15.1. p-tolyl 4-((3*R*,5*aS*,6*R*,8*aS*,9*S*,11*R*,11*aR*)-3,6,9-trimethyloctahydro-3*H*,11*H*-3,11-epoxy[1,2]dioxepino[3,4-*d*]isobenzofuran-9-carbonyl)piperazine-1-carboxylate (18a)

The product was obtained as white solid (112 mg, 66%), m.p.: 60.1-61.7°C. ¹H NMR (600 MHz, Chloroform-*d*) δ ppm: 7.16 (d, *J* = 8.2 Hz, 2H, Ph-3 and Ph-5), 6.98 (d, *J* = 8.4 Hz, 2H, Ph-2 and Ph-6), 5.73 (s, 1H, 12*a*-H), 4.23 (d, *J* = 52.4 Hz, 2H, piperazine-H), 3.64 (d, *J* = 50.0 Hz, 6H, piperazine-H), 2.40-2.30 (m, 5H), 2.09-1.99 (m, 2H), 1.89 (s, 3H, 3-CH₃), 1.55-1.49 (m, 2H), 1.46 (s, 3H, 9-CH₃), 1.43-1.19 (m, 3H), 1.05-0.99 (m, 2H), 0.98 (d, *J* = 6.4 Hz, 3H, 6-CH₃); ¹³C NMR (125 MHz, Chloroform-*d*) δ ppm: 172.69 (10-C=O), 153.93 (C=O), 148.93 (Ph-1), 135.08 (Ph-4), 129.84 (Ph-3 and Ph-5), 121.33 (Ph-2 and Ph-6), 103.84 (3-C), 97.35 (12*a*-C), 85.56 (12-C), 53.38 (9-C), 48.22 (5*a*-C), 45.97 (piperazine-C), 45.13 (piperazine-C), 44.51 (d, *J* = 8.0 Hz, piperazine-C), 43.95 (piperazine-C), 43.27 (8*a*-C), 37.14 (6-C), 37.05 (4-C), 32.49 (7-C), 27.73 (3-CH₃), 26.71 (9-CH₃), 25.26 (5-C), 24.66 (8-C), 20.84 (Ph-CH₃), 19.81 (6-CH₃). HRMS (ESI) *m/z* calcd. for [C₂₇H₃₆N₂O₇H⁺]: 501.2595, Found, 501.2561.

4.2.15.2. 4-fluorophenyl 4-((3*R*,5*aS*,6*R*,8*aS*,9*S*,11*R*,11*aR*)-3,6,9-trimethyloctahydro-3*H*,11*H*-3,11-epoxy[1,2]dioxepino[3,4-*d*]isobenzofuran-9-carbonyl)piperazine-1-carboxylate (18b)

The product was obtained as white solid (76 mg, 44%), m.p.: 85.9-90.7°C. ¹H NMR (500 MHz, Chloroform-*d*) δ ppm: 7.35-7.29 (m, 1H, Ph-H), 6.96-6.87 (m, 3H, Ph-H), 5.73 (s, 1H, 12*a*-H), 4.23 (d, *J* = 48.2 Hz, 2H, piperazine-H), 3.64 (d, *J* = 42.1 Hz, 6H, piperazine-H), 2.40-2.30 (m, 2H), 2.10-1.98 (m, 2H), 1.89 (s, 3H, 3-CH₃), 1.62-1.49 (m, 2H), 1.46 (s, 3H, 9-CH₃), 1.43-1.18 (m, 3H), 1.07-1.00 (m, 2H), 0.98 (d, *J* = 6.4 Hz, 3H, 6-CH₃); ¹³C NMR (125 MHz, Chloroform-*d*) δ ppm: 172.71 (10-C=O), 162.85 (d, *J* = 247.2 Hz, Ph-3), 153.09 (C=O), 152.04 (d, *J* = 10.9 Hz, Ph-1), 130.02 (d, *J* = 9.3 Hz, Ph-5), 117.41 (d, *J* = 10.9 Hz, Ph-6), 112.51 (d, *J* = 21.0 Hz, Ph-4), 109.78 (d, *J* = 24.2 Hz, Ph-2), 103.86 (3-C), 97.37 (12*a*-C), 85.55 (12-C), 53.39 (9-C), 48.21 (5*a*-C), 45.92 (piperazine-C), 45.23 (piperazine-C), 44.57 (d, *J* = 9.1 Hz, piperazine-C), 43.96 (piperazine-C), 43.21 (8*a*-C), 37.14 (6-C), 37.06 (4-C), 32.49 (7-C), 27.73 (3-CH₃), 26.72 (9-CH₃), 25.26 (5-C), 24.67 (8-C), 19.80 (6-CH₃). HRMS (ESI) *m/z* calcd. for [C₂₇H₃₃FN₂O₇H⁺]: 505.2345, Found, 505.2338.

4.2.15.3. 3-fluorophenyl 4-((3*R*,5*aS*,6*R*,8*aS*,9*S*,11*R*,11*aR*)-3,6,9-trimethyloctahydro-3*H*,11*H*-3,11-epoxy[1,2]dioxepino[3,4-*d*]isobenzofuran-9-carbonyl)piperazine-1-carboxylate (18c)

The product was obtained as white solid (76 mg, 44%), m.p.: 85.9-90.7°C. ¹H NMR (500 MHz, Chloroform-*d*) δ ppm: 7.35-7.29 (m, 1H, Ph-H), 6.96-6.87 (m, 3H, Ph-H), 5.73 (s, 1H, 12*a*-H), 4.23 (d, *J* = 48.2 Hz, 2H, piperazine-H), 3.64 (d, *J* = 42.1

Hz, 6H, piperazine-H), 2.40-2.30 (m, 2H), 2.10-1.98 (m, 2H), 1.89 (s, 3H, 3-CH₃), 1.62-1.49 (m, 2H), 1.46 (s, 3H, 9-CH₃), 1.43-1.18 (m, 3H), 1.07-1.00 (m, 2H), 0.98 (d, $J = 6.4$ Hz, 3H, 6-CH₃); ¹³C NMR (125 MHz, Chloroform-d) δ ppm: 172.71 (10-C=O), 162.85 (d, $J = 247.2$ Hz, Ph-3), 153.09 (C=O), 152.04 (d, $J = 10.9$ Hz, Ph-1), 130.02 (d, $J = 9.3$ Hz, Ph-5), 117.41 (d, $J = 10.9$ Hz, Ph-6), 112.51 (d, $J = 21.0$ Hz, Ph-4), 109.78 (d, $J = 24.2$ Hz, Ph-2), 103.86 (3-C), 97.37 (12a-C), 85.55 (12-C), 53.39 (9-C), 48.21 (5a-C), 45.92 (piperazine-C), 45.23 (piperazine-C), 44.57 (d, $J = 9.1$ Hz, piperazine-C), 43.96 (piperazine-C), 43.21 (8a-C), 37.14 (6-C), 37.06 (4-C), 32.49 (7-C), 27.73 (3-CH₃), 26.72 (9-CH₃), 25.26 (5-C), 24.67 (8-C), 19.80 (6-CH₃). HRMS (ESI) m/z calcd. for [C₂₇H₃₃FN₂O₇H⁺]: 505.2345, Found, 505.2338.

4.2.15.4. 2-fluorophenyl 4-((3*R*,5*aS*,6*R*,8*aS*,9*S*,11*R*,11*aR*)-3,6,9-trimethyloctahydro-3*H*,11*H*-3,11-epoxy[1,2]dioxepino[3,4-*d*]isobenzofuran-9-carbonyl)piperazine-1-carboxylate (18d)

The product was obtained as white solid (111 mg, 65%), m.p.: 65.2-66.3°C. ¹H NMR (600 MHz, Chloroform-d) δ ppm: 7.21-7.11 (m, 4H, Ph-H), 5.73 (s, 1H, 12a-H), 4.24 (d, $J = 59.7$ Hz, 2H, piperazine-H), 3.66 (d, $J = 64.2$ Hz, 6H, piperazine-H), 2.40-2.30 (m, 2H), 2.10-1.99 (m, 2H), 1.89 (s, 3H, 3-CH₃), 1.60-1.49 (m, 2H), 1.46 (s, 3H, 9-CH₃), 1.44-1.19 (m, 3H), 1.05-0.99 (m, 2H), 0.98 (d, $J = 6.4$ Hz, 3H, 6-CH₃); ¹³C NMR (125 MHz, Chloroform-d) δ ppm: 172.63 (10-C=O), 155.45 (d, $J = 248.3$ Hz, Ph-2), 152.71 (C=O), 138.69 (d, $J = 12.6$ Hz, Ph-1), 126.74 (d, $J = 7.1$ Hz, Ph-4), 124.37 (d, $J = 3.7$ Hz, Ph-5), 124.07 (Ph-6), 116.61 (d, $J = 18.4$ Hz, Ph-3), 103.85 (3-C), 97.36 (12a-C), 85.45 (12-C), 53.39 (9-C), 48.21 (5a-C), 45.92 (piperazine-C), 45.38 (piperazine-C), 44.75 (piperazine-C), 44.15 (piperazine-C), 43.21 (8a-C), 37.13 (6-C), 37.04 (4-C), 32.48 (7-C), 27.72 (3-CH₃), 26.70 (9-CH₃), 25.26 (5-C), 24.66 (8-C), 19.80 (6-CH₃). HRMS (ESI) m/z calcd. for [C₂₇H₃₃FN₂O₇H⁺]: 505.2345, Found, 505.2323.

4.2.15.5. 4-(trifluoromethyl)phenyl 4-((3*R*,5*aS*,6*R*,8*aS*,9*S*,11*R*,11*aR*)-3,6,9-trimethyloctahydro-3*H*,11*H*-3,11-epoxy[1,2]dioxepino[3,4-*d*]isobenzofuran-9-carbonyl)piperazine-1-carboxylate (18e)

The product was obtained as white solid (94 mg, 50%), m.p.: 119.9-122.7°C. ¹H NMR (600 MHz, Chloroform-d) δ ppm: 7.64 (d, $J = 8.6$ Hz, 2H, Ph-3 and Ph-5), 7.25 (d, $J = 8.6$ Hz, 2H, Ph-2 and Ph-6), 5.73 (s, 1H, 12a-H), 4.25 (d, $J = 71.4$ Hz, 2H, piperazine-H), 3.66 (d, $J = 54.1$ Hz, 6H, piperazine-H), 2.40-2.31 (m, 2H), 2.10-1.99 (m, 2H), 1.89 (s, 3H, 3-CH₃), 1.57-1.48 (m, 2H), 1.46 (s, 3H, 9-CH₃), 1.43-1.20 (m, 3H), 1.06-1.00 (m, 2H), 0.99 (d, $J = 6.4$ Hz, 3H, 6-CH₃); ¹³C NMR (125 MHz, Chloroform-d) δ ppm: 172.63 (10-C=O), 153.68 (Ph-1), 152.87 (C=O), 127.69 (q, $J = 32.8$ Hz, Ph-C), 126.70 (q, $J = 3.5$ Hz, Ph-C), 123.92 (q, $J = 270.4$ Hz, CF₃), 122.05 (Ph-C), 103.88 (3-C), 97.38 (12a-C), 85.55 (12-C), 53.38 (9-C), 48.19 (5a-C), 45.90 (piperazine-C), 45.28 (piperazine-C), 44.58 (piperazine-C), 43.99 (piperazine-C), 43.19 (8a-C), 37.12 (6-C), 37.06 (4-C), 32.48 (7-C), 27.73 (3-CH₃), 26.71 (9-CH₃), 25.25 (5-C), 24.66 (8-C), 19.80 (6-CH₃). HRMS (ESI) m/z calcd. for [C₂₇H₃₃F₃N₂O₇H⁺]: 555.2313, Found, 555.2317.

4.2.15.6. 3-(trifluoromethyl)phenyl 4-((3*R*,5*aS*,6*R*,8*aS*,9*S*,11*R*,11*aR*)-3,6,9-trimethyloctahydro-3*H*,11*H*-3,11-epoxy[1,2]dioxepino[3,4-*d*]isobenzofuran-9-

carbonyl)piperazine-1-carboxylate (18f)

The product was obtained as white solid (137 mg, 74%), m.p.: 132.0-136.7°C. ¹H NMR (600 MHz, Chloroform-d) δ ppm: 7.51-7.48 (m, 2H, Ph-4 and Ph-6), 7.40 (s, 1H, Ph-2) 7.33 (m, 1H, Ph-5), 5.74 (s, 1H, 12a-H), 4.25 (d, *J* = 68.4 Hz, 2H, piperazine-H), 3.66 (d, *J* = 62.4 Hz, 6H, piperazine-H), 2.41-2.30 (m, 2H), 2.11-1.99 (m, 2H), 1.89 (s, 3H, 3-CH₃), 1.60-1.49 (m, 2H), 1.46 (s, 3H, 9-CH₃), 1.42-1.19 (m, 3H), 1.06-1.00 (m, 2H), 0.99 (d, *J* = 6.4 Hz, 3H, 6-CH₃); ¹³C NMR (125 MHz, Chloroform-d) δ ppm: 172.76 (10-C=O), 153.03 (Ph-1), 151.24 (C=O), 131.83 (q, *J* = 33.0 Hz, Ph-C), 129.89 (Ph-C), 123.56 (q, *J* = 270.5 Hz, CF₃), 122.30 (q, *J* = 3.5 Hz, Ph-C), 118.98 (q, *J* = 3.5 Hz, Ph-C), 103.88 (3-C), 97.38 (12a-C), 85.55 (12-C), 53.39 (9-C), 48.20 (5a-C), 45.90 (piperazine-C), 45.24 (piperazine-C), 44.63 (d, *J* = 10.0 Hz, piperazine-C), 44.00 (piperazine-C), 43.19 (8a-C), 37.06 (6-C), 37.06 (4-C), 32.48 (7-C), 27.73 (3-CH₃), 26.72 (9-CH₃), 25.26 (5-C), 24.66 (8-C), 19.80 (6-CH₃). HRMS (ESI) m/z calcd. for [C₂₇H₃₃F₃N₂O₇H⁺]: 555.2313, Found, 555. 2317.

4.2.15.7. 3-(trifluoromethoxy)phenyl 4-((3*R*,5*aS*,6*R*,8*aS*,9*S*,11*R*,11*aR*)-3,6,9-trimethyloctahydro-3*H*,11*H*-3,11-epoxy[1,2]dioxepino[3,4-*d*]isobenzofuran-9-carbonyl)piperazine-1-carboxylate (18g)

The product was obtained as white solid (125 mg, 64%), m.p.: 113.3-117.9°C. ¹H NMR (600 MHz, Chloroform-d) δ ppm: 7.39 (t, *J* = 8.3 Hz, 1H, Ph-5), 7.10-7.07 (m, 2H, Ph-4 and Ph-6) 7.04 (s, 1H, Ph-2), 5.73 (s, 1H, 12a-H), 4.24 (d, *J* = 71.0 Hz, 2H, piperazine-H), 3.65 (d, *J* = 53.4 Hz, 6H, piperazine-H), 2.41-2.30 (m, 2H), 2.10-1.99 (m, 2H), 1.89 (s, 3H, 3-CH₃), 1.60-1.49 (m, 2H), 1.46 (s, 3H, 9-CH₃), 1.43-1.19 (m, 3H), 1.06-1.00 (m, 2H), 0.98 (d, *J* = 6.4 Hz, 3H, 6-CH₃); ¹³C NMR (125 MHz, Chloroform-d) δ ppm: 172.76(10-C=O), 152.95 (Ph-C), 151.83 (Ph-C), 149.48 (C=O), 130.02 (Ph-C), 120.38 (q, *J* = 256.0 Hz, OCF₃), 120.20 (Ph-C), 117.84 (Ph-C), 114.98 (Ph-C), 103.87(3-C), 97.38(12a-C), 85.55(12-C), 53.38(9-C), 48.20(5a-C), 45.90(piperazine-C), 45.26(piperazine-C), 44.61 (d, *J* = 12.8 Hz, piperazine-C), 44.02(piperazine-C), 43.19(8a-C), 37.05(6-C), 37.05(4-C), 32.48(7-C), 27.73(3-CH₃), 26.71(9-CH₃), 25.25(5-C), 24.66(8-C), 19.80(6-CH₃).HRMS (ESI) m/z calcd. for [C₂₇H₃₃F₃N₂O₈H⁺]: 571.2262, Found, 571.2275.

4.2.15.8. 4-((trifluoromethyl)thio)phenyl 4-((3*R*,5*aS*,6*R*,8*aS*,9*S*,11*R*,11*aR*)-3,6,9-trimethyloctahydro-3*H*,11*H*-3,11-epoxy[1,2]dioxepino[3,4-*d*]isobenzofuran-9-carbonyl)piperazine-1-carboxylate (18h)

The product was obtained as white solid (125 mg, 64%), m.p.: 113.3-117.9°C. ¹H NMR (600 MHz, Chloroform-d) δ ppm: 7.39 (t, *J* = 8.3 Hz, 1H, Ph-5), 7.10-7.07 (m, 2H, Ph-4 and Ph-6) 7.04 (s, 1H, Ph-2), 5.73 (s, 1H, 12a-H), 4.24 (d, *J* = 71.0 Hz, 2H, piperazine-H), 3.65 (d, *J* = 53.4 Hz, 6H, piperazine-H), 2.41-2.30 (m, 2H), 2.10-1.99 (m, 2H), 1.89 (s, 3H, 3-CH₃), 1.60-1.49 (m, 2H), 1.46 (s, 3H, 9-CH₃), 1.43-1.19 (m, 3H), 1.06-1.00 (m, 2H), 0.98 (d, *J* = 6.4 Hz, 3H, 6-CH₃); ¹³C NMR (125 MHz, Chloroform-d) δ ppm: 172.76 (10-C=O), 152.95 (Ph-C), 151.83 (Ph-C), 149.48 (C=O), 130.02 (Ph-C), 120.38 (q, *J* = 256.0 Hz, OCF₃), 120.20 (Ph-C), 117.84 (Ph-C), 114.98 (Ph-C), 103.87 (3-C), 97.38 (12a-C), 85.55 (12-C), 53.38 (9-C), 48.20 (5a-C), 45.90 (piperazine-C), 45.26 (piperazine-C), 44.61 (d, *J* = 12.8 Hz, piperazine-C), 44.02 (piperazine-C), 43.19 (8a-C), 37.05 (6-C), 37.05 (4-C), 32.48 (7-C), 27.73

(3-CH₃), 26.71 (9-CH₃), 25.25 (5-C), 24.66 (8-C), 19.80 (6-CH₃). HRMS (ESI) *m/z* calcd. for [C₂₇H₃₃F₃N₂O₈H⁺]: 571.2262, Found, 571.2275.

4.2.16. General procedure for the preparation of compounds (19a-19e)

Compound **17** (0.34 mmol) and HATU (0.41 mmol, 1.2equiv) was dissolved in 10 mL of DCM, and DIPEA (0.18 mmol, 3equiv) was added to the solution. The mixture was stirred for 1 h at room temperature, then the solution of compounds **7a-7e** in anhydrous tetrahydrofuran was added. The reaction mixture was stirred overnight at room temperature, then concentrated under reduced pressure and the residual was diluted by dichloromethane (30 mL). The mixture was extracted with DCM (3×30 mL) and the combined organic layer was washed with brine, dried over anhydrous Na₂SO₄ and evaporated to give crude product which was purified through column chromatography to afford compounds **19a-19e**.

4.2.16.1. N-(4-fluorophenyl)-4-((3*R*,5*aS*,6*R*,8*aS*,9*S*,11*R*,11*aR*)-3,6,9-trimethyloctahydro-3*H*,11*H*-3,11-epoxy[1,2]dioxepino[3,4-*d*]isobenzofuran-9-carbonyl)piperazine-1-carbothioamide (**19a**)

The product was obtained as white solid (80 mg, 45%), m.p.: 83.6-84.0°C. ¹H NMR (600 MHz, Chloroform-*d*) δ ppm: 7.20-7.16 (m, 2H, Ph-2 and Ph-6), 7.13 (s, 1H, NH), 7.08-7.04 (m, 2H, Ph-3 and Ph-5), 5.70 (s, 1H, 12*a*-H), 4.41 (s, 1H, piperazine-H), 4.03-3.65 (m, 7H, piperazine-H), 2.38-2.30 (m, 2H), 2.09-2.05 (m, 1H), 2.04-1.99 (m, 1H), 1.87 (s, 3H, 3-CH₃), 1.57-1.49 (m, 2H), 1.45 (s, 3H, 9-CH₃), 1.44-1.29 (m, 2H), 1.24-1.18 (m, 1H), 1.02 (d, *J* = 13.5 Hz, 1H), 0.98 (d, *J* = 6.4 Hz, 3H, 6-CH₃), 0.95 (d, *J* = 12.5 Hz, 1H); ¹³C NMR (125 MHz, Chloroform-*d*) δ ppm: 183.53 (C=S), 172.88 (10-C=O), 160.51 (d, *J* = 245.8 Hz, Ph-4), 135.65 (d, *J* = 3.1 Hz, Ph-1), 126.41 (d, *J* = 8.3 Hz, Ph-2 and Ph-6), 115.95 (d, *J* = 22.8 Hz, Ph-3 and Ph-5), 103.88 (3-C), 97.37 (12*a*-C), 85.53 (12-C), 53.30 (9-C), 48.85 (5*a*-C), 48.15 (d, *J* = 6.1 Hz, piperazine-C), 45.62 (piperazine-C), 45.05 (piperazine-C), 42.54 (8*a*-C), 37.10 (6-C), 37.01 (4-C), 32.44 (7-C), 27.63 (3-CH₃), 26.66 (9-CH₃), 25.24 (5-C), 24.62 (8-C), 19.79 (6-CH₃). HRMS (ESI) *m/z* calcd. for [C₂₆H₃₄FN₃O₅SH⁺]: 520.2276, Found, 520.2289.

4.2.16.2. N-(3-fluorophenyl)-4-((3*R*,5*aS*,6*R*,8*aS*,9*S*,11*R*,11*aR*)-3,6,9-trimethyloctahydro-3*H*,11*H*-3,11-epoxy[1,2]dioxepino[3,4-*d*]isobenzofuran-9-carbonyl)piperazine-1-carbothioamide (**19b**)

The product was obtained as white solid (58 mg, 33%), m.p.: 83.6-84.0°C. ¹H NMR (500 MHz, Chloroform-*d*) δ ppm: 7.56 (d, *J* = 33.2 Hz, 1H, Ph-H), 7.32-7.27 (m, Ph-H), 6.91 (dt, *J* = 16.5, 9.1 Hz, 2H, Ph-H), 5.70 (s, 1H, 12*a*-H), 4.47-3.59 (m, 8H, piperazine-H), 2.38-2.30 (m, 2H), 2.06-1.98 (m, 2H), 1.86 (s, 3H, 3-CH₃), 1.56-1.47 (m, 2H), 1.44 (s, 3H, 9-CH₃), 1.43-1.29 (m, 2H), 1.24-1.18 (m, 1H), 1.02 (d, *J* = 12.8 Hz, 1H), 0.98 (d, *J* = 6.4 Hz, 3H, 6-CH₃), 0.94 (d, *J* = 12.5 Hz, 1H); ¹³C NMR (125 MHz, Chloroform-*d*) δ ppm: 183.24 (C=S), 172.86 (10-C=O), 162.94 (d, *J* = 246.1 Hz, Ph-3), 141.41 (Ph-1), 130.32 (Ph-5), 118.74 (d, *J* = 9.3 Hz, Ph-6), 112.13 (d, *J* = 21.1 Hz, Ph-2), 110.45 (d, *J* = 25.2 Hz, Ph-4), 103.87 (3-C), 97.35 (12*a*-C), 85.54 (12-C), 53.30 (9-C), 49.43 (5*a*-C), 48.76 (piperazine-C), 48.20 (d, *J* = 3.7 Hz, piperazine-C), 45.66 (piperazine-C), 45.11 (piperazine-C), 42.58 (8*a*-C), 37.11 (6-C),

37.00 (4-C), 32.44 (7-C), 27.63 (3-CH₃), 26.65 (9-CH₃), 25.24 (5-C), 24.62 (8-C), 19.79 (6-CH₃). HRMS (ESI) *m/z* calcd. for [C₂₆H₃₄FN₃O₅SH⁺]: 520.2276, Found, 520.2250.

4.2.16.3. N-(2-fluorophenyl)-4-((3*R*,5*aS*,6*R*,8*aS*,9*S*,11*R*,11*aR*)-3,6,9-trimethyloctahydro-3*H*,11*H*-3,11-epoxy[1,2]dioxepino[3,4-*d*]isobenzofuran-9-carbonyl)piperazine-1-carbothioamide (19c)

The product was obtained as white solid (57 mg, 32%), m.p.: 106.5-109.3°C. ¹H NMR (500 MHz, Chloroform-*d*) δ ppm: 7.61 (t, *J* = 7.9 Hz, 1H, Ph-H), 7.19-7.08 (m, 3H, Ph-H), 5.71 (s, 1H, 12a-H), 4.49-3.59 (m, 8H, piperazine-H), 2.38-2.29 (m, 2H), 2.11-2.05 (m, 1H), 2.03-1.98 (m, 1H), 1.86 (s, 3H, 3-CH₃), 1.59-1.48 (m, 2H), 1.45 (s, 3H, 9-CH₃), 1.42-1.29 (m, 2H), 1.24-1.18 (m, 1H), 1.03 (d, *J* = 13.2 Hz, 1H), 0.98 (d, *J* = 6.4 Hz, 3H, 6-CH₃), 0.93 (d, *J* = 13.0 Hz, 1H); ¹³C NMR (125 MHz, Chloroform-*d*) δ ppm: 182.83 (C=S), 172.89 (10-C=O), 155.10 (d, *J* = 246.1 Hz, Ph-2), 127.53 (d, *J* = 11.2 Hz, Ph-5), 126.62 (d, *J* = 7.7 Hz, Ph-4), 126.09 (Ph-6), 124.18 (d, *J* = 3.7 Hz, Ph-1), 115.82 (d, *J* = 19.7 Hz, Ph-3), 103.87 (3-C), 97.39 (12a-C), 85.53 (12-C), 53.33 (9-C), 48.75 (5a-C), 48.14 (d, *J* = 14.8 Hz, piperazine-C), 45.59 (piperazine-C), 45.02 (piperazine-C), 42.51 (8a-C), 37.12 (6-C), 37.02 (4-C), 32.45 (7-C), 27.65 (3-CH₃), 26.68 (9-CH₃), 25.24 (5-C), 24.63 (8-C), 19.79 (6-CH₃). HRMS (ESI) *m/z* calcd. for [C₂₆H₃₄FN₃O₅SH⁺]: 520.2276, Found, 520.2282.

4.2.16.4. N-(3-(trifluoromethyl)phenyl)-4-((3*R*,5*aS*,6*R*,8*aS*,9*S*,11*R*,11*aR*)-3,6,9-trimethyloctahydro-3*H*,11*H*-3,11-epoxy[1,2]dioxepino[3,4-*d*]isobenzofuran-9-carbonyl)piperazine-1-carbothioamide (19d)

The product was obtained as white solid (53 mg, 27%), m.p.: 119.8-126.4°C. ¹H NMR (500 MHz, Chloroform-*d*) δ ppm: 7.60 (s, 1H, NH), 7.47-7.41 (m, 4H, Ph-H), 5.69 (s, 1H, 12a-H), 4.42 (s, 1H, piperazine-H), 4.10-3.64 (m, 7H, piperazine-H), 2.37-2.28 (m, 2H), 2.06-1.97 (m, 2H), 1.86 (s, 3H, 3-CH₃), 1.56-1.46 (m, 2H), 1.44 (s, 3H, 9-CH₃), 1.41-1.30 (m, 2H), 1.23-1.17 (m, 1H), 1.02 (d, *J* = 13.3 Hz, 1H), 0.97 (d, *J* = 6.3 Hz, 3H, 6-CH₃), 0.94 (d, *J* = 15.1 Hz, 1H); ¹³C NMR (125 MHz, Chloroform-*d*) δ ppm: 182.80 (C=S), 172.96 (10-C=O), 140.28 (Ph-1), 131.45 (q, *J* = 32.4 Hz, Ph-C), 129.54 (Ph-C), 126.99 (Ph-C), 123.71 (q, *J* = 270.6 Hz, CF₃), 121.96 (q, *J* = 3.5 Hz, Ph-C), 120.22 (q, *J* = 3.6 Hz, Ph-C), 103.89 (3-C), 97.35 (12a-C), 85.54 (12-C), 53.28 (9-C), 49.11 (5a-C), 48.40 (piperazine-C), 48.16 (piperazine-C), 45.07 (piperazine-C), 42.56 (8a-C), 37.09 (6-C), 36.98 (4-C), 32.41 (7-C), 27.59 (3-CH₃), 26.63 (9-CH₃), 25.22 (5-C), 24.61 (8-C), 19.77 (6-CH₃). HRMS (ESI) *m/z* calcd. for [C₂₇H₃₄F₃N₃O₅SH⁺]: 570.2244, Found, 570.2239.

4.2.16.5. N-(4-(trifluoromethyl)phenyl)-4-((3*R*,5*aS*,6*R*,8*aS*,9*S*,11*R*,11*aR*)-3,6,9-trimethyloctahydro-3*H*,11*H*-3,11-epoxy[1,2]dioxepino[3,4-*d*]isobenzofuran-9-carbonyl)piperazine-1-carbothioamide (19e)

The product was obtained as white solid (72 mg, 37%), m.p.: 160.6-166.4°C. ¹H NMR (600 MHz, Chloroform-*d*) δ ppm: 7.60 (d, *J* = 8.5 Hz, 2H, Ph-3 and Ph-5), 7.29 (d, *J* = 8.6 Hz, 2H, Ph-2 and Ph-6), 5.70 (s, 1H, 12a-H), 4.43 (s, 1H, piperazine-H), 4.16-3.59 (m, 7H, piperazine-H), 2.38-2.29 (m, 2H), 2.10-1.98 (m, 2H), 1.87 (s, 3H, 3-CH₃), 1.58-1.49 (m, 2H), 1.44 (s, 3H, 9-CH₃), 1.41-1.16 (m, 3H), 1.02 (d, *J* = 15.6

Hz, 1H), 0.98 (d, $J = 6.4$ Hz, 3H, 6-CH₃), 0.94 (d, $J = 12.8$ Hz, 1H); ¹³C NMR (125 MHz, Chloroform-d) δ ppm: 182.95 (C=S), 172.91 (10-C=O), 142.79 (Ph-1), 126.86 (q, $J = 32.8$ Hz, Ph-C), 126.34 (q, $J = 3.6$ Hz, Ph-C), 123.94 (q, $J = 270.1$ Hz, CF₃), 122.55 (Ph-C), 103.89 (3-C), 97.37 (12a-C), 85.52 (12-C), 53.29 (9-C), 49.40 (5a-C), 48.71 (piperazine-C), 48.18 (d, $J = 5.5$ Hz, piperazine-C), 45.09 (piperazine-C), 42.57 (8a-C), 37.09 (6-C), 37.01 (4-C), 32.43 (7-C), 27.64 (3-CH₃), 26.66 (9-CH₃), 25.23 (5-C), 24.62 (8-C), 19.78 (6-CH₃). HRMS (ESI) m/z calcd. for [C₂₇H₃₄F₃N₃O₅SH⁺]: 570.2244, Found, 570.2235.

4.3. Cell culture and drug treatment in general

All the cell lines were purchased from Shanghai BiopalCo, Ltd (Shanghai, China). MCF-7, A549, HCT-116, PC-12, U87MG, U-118MG and L02 (STR report in the supplementary materials) were cultured in DMEM medium supplemented with 10% FBS and 1% penicillin/streptomycin. SH-SY5Y cells were cultured in DMEM/F12 medium supplemented with 10% FBS and 1% penicillin/streptomycin. All the cells were incubated at 37°C, 5% CO₂ in a humidified atmosphere.

Cells were treated with the chemicals at different concentrations (e.g., 0, 1, 2, 4 μ M, etc.) for various time (e.g., 12, 24 or 48 h) according to the targets we examined and the corresponding analysis methods to get better contrast with the controls.

4.4. Cell viability assay

Cell viability was determined by MTT assay (Beyotime, Jiangsu, China). Compounds were dissolved in DMSO and diluted with culture medium. Briefly, cells (4×10^3 in 100 μ L) were seeded in 96-well plates. After incubation for 24 h, the medium was removed and replaced by fresh medium containing derivatives at various concentrations for 72 h at 37°C. The medium containing derivatives was then replaced with 100 μ L serum-free medium containing 0.5 mg/mL MTT for 4 h incubation. The MTT solution was removed and 100 μ L/well of DMSO was added to dissolve the formazan. The absorbance was measured using a 96-well plate reader (SH-1000 Lab, Corona Electric, Japan) at 490 nm. Cell inhibition rate (%) = $(1 - A_{490\text{sample}}/A_{490\text{control}}) \times 100\%$. IC₅₀ values were calculated by GraphPad Prism 6. All experiments were performed in three biological replicates.

4.5. Cell cycle assay

HCT-116 cells were seeded in 6-well plates at the density of 1×10^5 cells/well and treated with different concentrations (0, 1, 2 and 4 μ M) of compound **12h** formulated by 3% medium for 24 h at growth conditions. Cells were collected and washed with PBS, centrifuged at 2500 rpm/min for 4 min, then fixed with 70% ethanol and incubated at 4°C overnight. Cell Cycle and Apoptosis Analysis Kit (Beyotime, Jiangsu, China) was used to determine cell cycle. Cells were then centrifuged at 2500 rpm for 4 min and washed with PBS, the pellet was resuspended in 500 μ L dye binding solution and incubated with RNase A (50 μ g/mL) and PI (20X) at 37°C for 30 min. Samples were analyzed using a flow cytometer (Accuri C6 Plus, BD Biosciences, USA).

4.6. Cell apoptosis assay

4.6.1. Annexin V/PI detection

Annexin V-FITC Apoptosis Detection Kit (Beyotime, Jiangsu, China) was used to determine cell apoptosis induced by compound **12h**. 1×10^5 cells were seeded per well in 6-well plates. After treatment with or without desired concentrations of **12h** (0.25, 0.5, 1, 2 and 4 μM) for 24 h, cells were collected and washed with cold PBS. Each sample containing 2×10^5 cells was centrifuged at 2000 rpm for 4 min. Cells were stained with annexin-V-fluorescein isothiocyanate (FITC) and PI in binding buffer for 20 min at room temperature in the dark and washed twice with cold PBS. The apoptotic cells were determined by flow cytometry. Cells undergoing early and late apoptosis were labeled by annexin-V, and both annexin-V and PI, respectively.

4.6.2. Hoechst 33258 staining

HCT-116 cells were treated for 48 h with compound **12h** at concentrations of 0.25, 0.5, 1, 2 and 4 μM and stained with 5 $\mu\text{g}/\text{mL}$ Hoechst 33258 (Beyotime, Jiangsu, China) for 20 min at growth conditions. The morphological changes of apoptotic cells in nuclei and nuclear chromatin were determined using a fluorescence microscope (XD20-RFL, Ningboshunyu, China).

4.7. Mitochondrial membrane potential assay

Cationic lipophilic dye JC-1 probe (Beyotime, Haimen, China) was used to determine mitochondrial membrane potential ($\Delta\Psi\text{m}$). HCT-116 cells were treated with **12h** at concentrations of 0.5, 1 and 2 μM for 48 h, incubated with an equal volume of JC-1 staining solution (5 $\mu\text{g}/\text{mL}$) at 37°C for 25 min and then rinsed twice with PBS. The changes of $\Delta\Psi\text{m}$ were monitored by determining the relative amounts of dual emissions from mitochondrial JC-1 monomers or aggregates under the XD20-RFL fluorescent microscope. Mitochondrial depolarization is indicated by an increase in the green/red fluorescence intensity ratio. The excitation and emission wavelength were 514 nm and 515–545 nm (green) for JC-1 monomer; 585 nm and 570–600 nm (red) for J- aggregates.

We quantified of $\Delta\Psi\text{m}$ in HCT-116 cells using TMER assay kit (Abcam, UK). 1×10^5 cells were seeded per well in the 6-well plates and treated with **12h** at concentrations of 0.25, 0.5, 1, 2 and 4 μM for 48 h. Cells were collected and washed with PBS. 500 μL working TMER solution (50 nM) was added to each sample before incubation for 25 min at 37°C. The stained cells were washed twice with serum-free medium by centrifugation at 2000 rpm for 5 min. $\Delta\Psi\text{m}$ was measured by flow cytometry as mean fluorescence intensity.

4.8. ROS assay

DCFH-DA assay kit (Beyotime, Haimen, China) was used to quantify the intracellular reactive oxygen species (ROS) levels in HCT-116 cells. Cells were treated with **12h** at concentrations of 0.5, 1, 2, 4 and 8 μM for 12 h, washed and incubated with DCFH-DA (2.5 μM) at 37°C for 20 min. The stained cells were

washed twice with serum-free medium by centrifugation at 2000 rpm for 5 min. Cellular fluorescence was measured by flow cytometry. The enhanced fluorescence compared to the control represents the increase of intracellular ROS levels.

4.9. Intracellular free calcium levels assay

The intracellular free calcium levels were quantified by Ca²⁺ indicator dye Fluo-3AM (Beyotime, Haimen, China). Cells pretreated with **12h** at concentrations of 0.25, 0.5, 1 and 2 μ M for 24 h were washed with PBS and incubated with Fluo-3AM (5 μ M) for 50 min. Samples were washed twice and incubated with PBS for 15 minutes before analysis by flow cytometry.

4.10. Western blotting analysis

HCT-116 cells were cultured for 24 h in the 100 mm cell culture dish, treated with different concentrations of **12h** (0, 0.125 and 0.25 μ M) for 48 h and scraped down with a cell scraper. The total cellular protein was extracted by RIPA lysis buffer with protease inhibitor (Beyotime, Jiangsu, China). The protein concentration was quantified using the BCA Protein Assay Reagent (Beyotime, Jiangsu, China). Total protein (50 μ g) was separated by sodium dodecylsulfate-polyacrylamide electrophoresis gels (SDS-PAGE) and transferred to polyvinylidene fluoride (PVDF) membrane. The membranes were washed three times with 1 \times Tris-buffered saline containing 0.1% Tween 20 (TBST), blocked with 5% fat-free milk in 1 \times TBST overnight at room temperature. The membranes were incubated with Bax, Bcl-2, caspase-3, cleaved caspase-9, and β -actin antibodies (1:2000 in 5% fat-free milk, Cell Signaling Technology, USA) at 4°C overnight and then washed three times with 1 \times TBST. Secondary antibodies of horseradish-peroxidase-conjugated anti-rabbit IgG (1:3000 in 5% fat-free milk, Cell Signaling Technology, USA) were added before incubation for 3 hours using a shaker. The immune reactive band was visualized with ECL-detecting reagents. ImageJ software was used for picture analysis.

4.11. Cell migration assay

The scratch test was carried out to verify the inhibition of cell migration. HCT-116 cells were cultured in 6-well plates for 24 h before scratches were made in the confluent monolayers by a 20 μ L pipette tip. Wounds were washed twice with PBS to remove detached cell debris. The medium containing different concentrations (0, 0.25, 0.5, 1 and 2 μ M) of the compound **12h** were added to the plates. Cells which migrated across the wound area were photographed by microscopy (Mshot, China) at 0 and 24 h. The migration distance to the wound area was measured manually.

4.12. Anti-vascular activity assay

EC Matrigel matrix (Corning, USA) was melted at 4°C, added to the 96-well culture plate (60 μ L/well) and polymerized at 37°C for 30 min, before primary human umbilical vein endothelial cells (HUVEC) suspended in ECM were seeded in the plate (2 \times 10⁴ cells/well). Cells were treated with 100 μ L of different concentrations of compound **12h** (0, 0.5, 1, 2 and 4 μ M) for 24 h at 37°C. The morphological changes

of the cells and tubes were observed and photographed by microscopy (Mshot, China).

4.13. Statistical analysis

Three biological replicates were performed in the experiments and used for calculation of experimental means and standard deviations. One-way ANOVA was applied to the data. Values of $p < 0.05$ were interpreted as significant.

Conflict of interest

The authors declare no competing financial interest or personal relationships that could have appeared to influence the work reported in this paper.

Acknowledgements

We thanks for the financial support from the Doctorate Startup Fund of Southwest University of Science and Technology (18ZX713001); National Natural Science Foundation of China (11705170); Foundation from Institute of Materials CAEP (TP02201709).

Reference

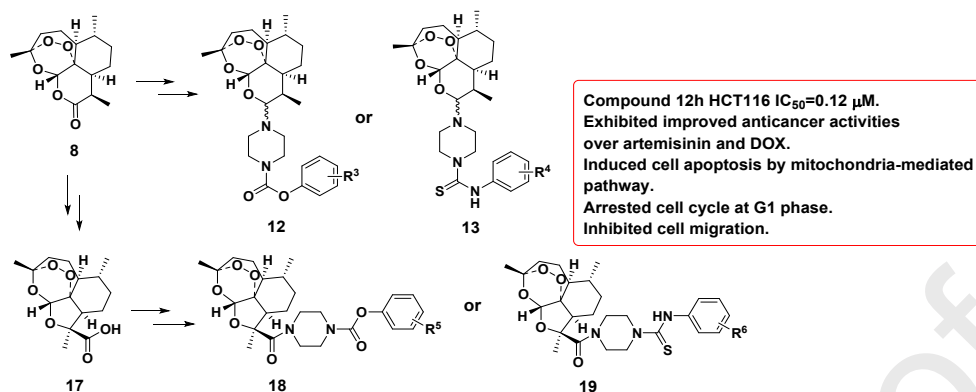
- [1] Y. Tu, Artemisinin—A Gift from Traditional Chinese Medicine to the World (Nobel Lecture). *Angewandte Chemie International Edition* 55 (2016), 10210-10226.
- [2] P.M. O'Neill, V.E. Barton, S.A. Ward, The Molecular Mechanism of Action of Artemisinin—The Debate Continues. *Molecules*. 15 (2010), 1705-1721.
- [3] R.X. Tan, W.F. Zheng, H.Q. Tang, Biologically active substances from the genus artemisia. *Planta Medica*. 64 (1998), 295-302.
- [4] S. Appalasamy, K.Y. Lo, S.J. Chng, K. Nornadia, A.S. Othman, L. Chan, Antimicrobial activity of artemisinin and precursor derived from in vitro plantlets of artemisia annua L. *BioMed Research International*. 2014 (2014), 215872-215872.
- [5] W. Kim, W.J. Choi, S. Lee, W.J. Kim, D.C. Lee, U.D. Sohn, H. Shin, W. Kim, Anti-inflammatory, antioxidant and antimicrobial effects of artemisinin extracts from artemisia annua L. *The Korean Journal of Physiology and Pharmacology*. 19 (2014), 21-27.
- [6] X. Wang, B. Zheng, U. Ashraf, H. Zhang, J. Ye, Artemisinin inhibits the replication of flaviviruses by promoting the type I interferon production. *Antiviral Research*. 179 (2020), 104810.
- [7] J. Yu, X. Li, M. Wei, Synthesis and biological activities of artemisinin-piperazine-dithiocarbamate derivatives. *European Journal of Medicinal Chemistry*. 169 (2019), 21-28.
- [8] X.Y. Gu, Y.Y. Peng, Y.Y. Zhao, X. Liang, Y. Tang, J.W. Liu, A novel derivative of artemisinin inhibits cell proliferation and metastasis via down-regulation of cathepsin K in breast cancer. *European Journal of*

- Pharmacology*. 858 (2019), 172382.
- [9] G.E. Magoulas, T. Tsigkou, L. Skondra, M. Lamprou, E. Papadimitriou, Synthesis of novel artemisinin simers with polyamine linkers and evaluation of their potential as anticancer agents. *Bioorganic & Medicinal Chemistry Letters*. 25 (2017), 3756-3767.
- [10] Y. Yang, X. Zhang, X. Wang, X. Zhao, T. Ren, F. Wang, B. Yu, Enhanced delivery of artemisinin and its analogues to cancer cell line by their adducts with human serum transferrin, *International Journal of Pharmaceutics*. 467 (2014), 113-122.
- [11] T.T. Cloete, C.De. Kock, P.J. Smith, D.D. Nda, Synthesis, in vitro antiplasmodial activity and cytotoxicity of a series of artemisinin-triazine hybrids and hybrid-dimers. *European Journal of Medicinal Chemistry*. 76 (2014), 470-481.
- [12] S. Jana, S. Iram, J. Thomas, S. Liekens, W. Dehaen, Synthesis and anticancer activity of novel aza-artemisinin derivatives. *Bioorganic & Medicinal Chemistry*. 25 (2017), 3671-3676.
- [13] A.F. Britoa, L.K.S. Moreiraa, R. Menegattib, E.A. Costa, Piperazine derivatives with central pharmacological activity used as therapeutic tools. *Fundamental & clinical pharmacology*. 33 (2019), 13-24.
- [14] Q. Sun, J. Wang, Y. Li, J.J. Zhuang, Q. Zhang, X. Sun, D.Q. Sun, Synthesis and evaluation of cytotoxic activities of artemisinin derivatives. *Chemical Biology & Drug Design*. 90 (2017), 1019-1028.
- [15] M. Li, X. Xue, J. Cheng, Establishing cation and radical donor ability scales of electrophilic F, CF₃, and SCF₃ transfer reagents. *Accounts of Chemical Research*. 53 (2020), 182-197.
- [16] E.P. Gillis, K.J. Eastman, M.D. Hill, D.J. Donnelly, N.A. Meanwell, applications of fluorine in medicinal chemistry. *Journal of Medicinal Chemistry*. 58 (2015), 8315-8359.
- [17] C. Heidelberger, N.K. Chaudhuri, P.B. Danneberg, D. Mooren, L. Griesbach, R. Duschinsky, R.J. Schnitzer, E. Plevin, J. Scheiner, Fluorinated pyrimidines, a new class of tumour-inhibitory compounds. *Nature*. 179 (1957), 663-666.
- [18] G. Li, Q. Sun, D. Wang, Y. Xu, J.J. Zhuang, Q. Zhang, D.Q. Sun, Fluoroalkane thioheterocyclic derivatives and their antitumor activity. *European Journal of Medicinal Chemistry*. 93 (2015), 423-430.
- [19] F. Grellepois, F. Chorki, M. Ourevitch, S. Charneau, P. Grellier, K.A. McIntosh, W.N. Charman, B. Pradines, B. Crousse, D. Bonnetdelpon, Orally active antimalarials: hydrolytically stable derivatives of 10-trifluoromethyl anhydrodihydroartemisinin †. *Journal of Medicinal Chemistry*. 47 (2004), 1423-1433.
- [20] S. Li, G. Li, X. Yang, Q. Meng, S. Yuan, Y. He, D.Q. Sun, Design, synthesis and biological evaluation of artemisinin derivatives containing fluorine atoms as anticancer agents. *Bioorganic & Medicinal Chemistry Letters*. 28 (2018), 2275-2278.
- [21] N. Zhang, Z. Yu, X. Yang, P. Hu, Y. He, Synthesis of novel ring-contracted

- artemisinin dimers with potent anticancer activities. *European Journal of Medicinal Chemistry*. 150 (2018), 829-840.
- [22] H. Sun, X. Meng, J. Han, Z. Zhang, B. Wang, X. Bai, X. Zhang, Anti-cancer activity of DHA on gastric cancer—an in vitro and in vivo study. *Tumor Biology*, 34 (2013), 3791-3800.
- [23] Y.B. Wang, H. Yi, L. Zhen, W. Ping, Y.X. Xue, Y.L. Yao, B. Yun, H.Y. Liu, Artemether combined with shRNA interference of vascular cell adhesion molecule-1 significantly inhibited the malignant biological behavior of human glioma cells. *Plos One*. 8 (2013), e60834.
- [24] G.Q. Qin, C.B. Zhao, L.L. Zhang, H.Y. Liu, Y.Y. Quan, L.Y. Chai, S.G. Wu, X.P. Wang, T.S. Chen, Dihydroartemisinin induces apoptosis preferentially via a bim-mediated intrinsic pathway in hepatocarcinoma cells. *Apoptosis*. 20 (2015), 1072-1086.
- [25] L.L. Wang, L. Kong, H. Liu, Y. Zhang, L. Zhang, X. Liu, F. Yuan, Y. Li, Z. Zuo, Design and synthesis of novel artemisinin derivatives with potent activities against colorectal cancer in vitro and in vivo. *European Journal of Medicinal Chemistry*. 182 (2019), 111665.
- [26] S. Krishna, S. Ganapathi, I.C. Ster, M.E.M. Saeed, M. Cowan, C. Finlayson, H. Kovacsevics, H. Jansen, P.G. Kremsner, T. Efferth, A randomised, double blind, placebo-controlled pilot study of oral artesunate therapy for colorectal cancer. *EBioMedicine*. 2 (2015), 82-90.
- [27] Y. Venkatesh, S. Nandi, M. Shee, B. Saha, A. Anoop, N.D.P. Singh, Bis - acetyl carbazole: a photoremovable protecting group for sequential release of two different functional groups and its application in therapeutic release. *European Journal of Organic Chemistry*. 2017 (2017), 6121-6130.
- [28] C. Ren, K. Morohashi, A.N. Plotnikov, J. Jakoncic, S.G. Smith, J. Li, L. Zeng, Y. Rodriguez, V. Stojanoff, M.J. Walsh, Small-Molecule modulators of methyl-lysine binding for the CBX7 chromodomain. *Chemistry & Biology*. 22 (2015), 161-168.
- [29] J.Z. Long, X. Jin, A. Adibekian, W. Li, B.F. Cravatt, Characterization of tunable piperidine and piperazine carbamates as inhibitors of endocannabinoid hydrolases. *Journal of Medicinal Chemistry*. 53 (2010), 1830-1842.
- [30] R. Zhuang, L. Gao, X. Lv, J. Xi, L. Sheng, Y. Zhao, R. He, X. Hu, Y. Shao, X. Pan, Exploration of novel piperazine or piperidine constructed non-covalent peptidyl derivatives as proteasome inhibitors. *European Journal of Medicinal Chemistry*. 126 (2017), 1056-1070.
- [31] L. Xi, J. Zhang, Z. Liu, J. Zhang, J. Yan, Y. Jin, J. Lin, Novel 5-anilinoquinazoline-8-nitro derivatives as inhibitors of VEGFR-2 tyrosine kinase: synthesis, biological evaluation and molecular docking. *Organic and Biomolecular Chemistry*. 11 (2013), 4367-4378.
- [32] J. Sánchez Céspedes, P. Martínez-Aguado, M. Vega-Holm, A. Serna-Gallego, J.I. Candela, J.A. Marrugal-Lorenzo, J. Pachón, F. Iglesias-Guerra, J.M. Vega-Pérez, New 4-Acyl-1-phenylaminocarbonyl-2-phenylpiperazine derivatives as potential inhibitors of adenovirus infection. Synthesis,

- biological evaluation, and structure–activity relationships. *Journal of Medicinal Chemistry*. 59 (2016), 5432-5448.
- [33] J.D. Steyn, L. Wiesner, L.H.D. Plessis, A.F. Grobler, P.J. Smith, W.C. Chan, R.K. Haynes, A.F. Kotzé, Absorption of the novel artemisinin derivatives artemisone and artemiside: potential application of Pheroid technology. *International Journal of Pharmaceutics*. 414 (2011), 260-266.
- [34] J. Zhang, R. Huang, H. Cao, A. Cheng, C. Jiang, Z. Liao, C. Liu, J. Sun, Chemical composition, in vitro anti-tumor activities and related mechanisms of the essential oil from the roots of *Potentilla discolor*. *Industrial Crops and Products*. 113 (2018), 19-27.
- [35] J. Lewerenz, G. Ates, A. Methner, M. Conrad, P. Maher, Oxytosis/Ferroptosis-(Re-) emerging roles for oxidative stress-dependent non-apoptotic cell death in diseases of the central nervous system. *Frontiers in Neuroscience*. 12 (2018), 214.
- [36] Y. Shi, A structural view of mitochondria-mediated apoptosis. *Nature Structural & Molecular Biology*. 8 (2001), 394-401.
- [37] X. Liu, C.N. Kim, J. Yang, R. Jemmerson, X. Wang, Induction of apoptotic program in cell-free extracts: requirement for dATP and cytochrome c. *Cell*. 86 (1996), 147-157.
- [38] A.W. Konradi, M.A. Pleiss, C.M. Semko, T. Yednock, J.L. Smith, Multivalent VLA-4 antagonists comprising polymer moieties. E.P. Patent. 2010, 2258399A2.
- [39] A.L. Zulli, L.D. Aimone, J.R. Mathiasen, J.A. Gruner, R. Raddatz, E.R. Bacon, R.L. Hudkins, Substituted phenoxypropyl-(R)-2-methylpyrrolidine aminomethyl ketones as histamine-3 receptor inverse agonists. *Bioorganic & Medicinal Chemistry Letters*. 22 (2012), 2807-2810.
- [40] J. Sánchez Céspedes, M.E. Pachón Ibáñez, J. Pachón Díaz, P. Martínez Aguado, T. Cebrero Canguero, J.M. Vega Pérez, F. Iglesias Guerra, M. Vega Holm, J.I. Candela Lena, S. Mazzotta, Piperazine derivatives as antiviral agent with increased therapeutic activity. *Patent*. 2017, 2017144624.

Graphical Abstract



Highlights

- A series of novel artemisinin derivatives containing piperazine and fluorine groups were designed and synthesized.
- The anti-tumor activities of most compounds were better than ART and DHA in six cancer cell lines with lower cytotoxicity in normal cell line (L02). Especially, the activity of two compounds **12g** and **12h** was comparable to or higher than that of DOX, with lower toxicity.
- The preliminary structure-activity relationship (SAR) was summarized based on our work.
- Compound **12h** showed the best activity against HCT-116 cell line with an IC_{50} of 0.12 μ M, and low toxicity against normal cell line L02 with an IC_{50} of 12.46 μ M.
- The mechanisms of artemisinin derivatives against colorectal cancer were studied.
- Compound **12h** arrested the cell cycle in the G1 phase, inhibited HCT-116 cells migration and induced apoptosis by the mitochondria-mediated pathway.

Declaration of interests

The authors declare no competing financial interest or personal relationships that could have appeared to influence the work reported in this paper.

Journal Pre-proofs